Mon. Not. R. Astron. Soc. **000**, 1–20 (2001) Printed 2 February 2008 (MN LaTeX style file v1.4)

Stationary Nonaxisymmetric Configurations of Magnetized Singular Isothermal Disks

Yu-Qing Lou[1]
[1] *National Astronomical Observatories, Chinese Academy of Sciences, A20, Datun Road, Beijing, 100012 China;*
Department of Astronomy and Astrophysics, The University of Chicago, Chicago, Illinois 60637 USA;
Email: lou@oddjob.uchicago.edu; and
Physics Department, The Tsinghua Astrophysics Center, Tsinghua University, Beijing 100084 China.

Accepted .... Received ...; in original form ...

ABSTRACT
We construct both aligned and unaligned (logarithmic spiral) stationary configurations of nonaxisymmetric magnetohydrodynamic (MHD) disks from either a full or a partial razor-thin power-law axisymmetric magnetized singular isothermal disk (MSID) that is embedded with a coplanar azimuthal magnetic field B_θ of a non-force-free radial scaling $r^{-1/2}$ and that rotates differentially with a flat rotation curve of speed aD, where a is the isothermal sound speed and D is the dimensionless rotation parameter. Analytical solutions and stability criteria for determining D^2 are derived. For aligned nonaxisymmetric MSIDs, eccentric $m=1$ displacements may occur at arbitrary D^2 in a full MSID but are allowed only with $a^2D^2=C_A^2/2$ in a partial MSID (C_A is the Alfvén speed), while each case of $|m|\geq 1$ gives two possible values of D^2 for purely azimuthal propagations of fast and slow MHD density waves (FMDWs and SMDWs) that appear stationary in an inertial frame of reference. For disk galaxies modeled by a partial MSID resulting from a massive dark-matter halo with a flat rotation curve and $a^2D^2\gg C_A^2$, stationary aligned perturbations of $m=1$ are not allowed. For unaligned logarithmic spiral MSIDs with $|m|\geq 1$, there exist again two values of D^2, corresponding to FMDWs and SMDWs that propagate in both radial and azimuthal directions relative to the MSID and that appear stationary in an inertial frame of reference. The larger D^2 is always physically valid, while the smaller D^2 is valid only for $a>C_A/2$ with a positive surface mass density Σ_0. For observational diagnostics, we examine the spatial phase relationships among enhancements of gas density and magnetic field as well as velocity perturbations. These results are useful for probing magnetized bars, or lopsided, normal, and barred spiral galaxies as well as for testing numerical MHD codes. In the case of NGC 6946, interlaced optical and magnetic field spiral patterns of SMDWs can persist in a disk of flat rotation curve. Theoretical issues regarding the modal formalism and the MSID perspective are also discussed.

Key words: accretion, accretion disks — galaxies: evolution — galaxies: magnetic fields — galaxies: barred, spiral — ISM: magnetic fields — MHD

1 INTRODUCTION

It is a challenge to study the large-scale dynamics of various morphologies of disk galaxies such as bars and lopsided, barred, and normal spiral structures (e.g., Baldwin, Lynden-Bell, & Sancisi 1980; Richter & Sancisi 1994; Rix & Zaritsky 1995). To include gravitational interactions and magnetohydrodynamics (MHD) of the interstellar medium (ISM) and magnetic field, we risk in making the task even more formidable. However, multi-wavelength observational diagnostics involving both ISM and magnetic field do provide indispensable clues to the overall dynamics. For example, there have been growing numbers of high-quality observations on large-scale magnetic field structures in nearby spiral galaxies (e.g., Sofue et al. 1986; Kronberg 1994; Beck et al. 1996; Beck 2001 and references therein). We here venture to formulate a limited yet nontrivial theoretical MHD disk problem in which stationary nonaxisymmetric MHD perturbation configurations are constructed from a background axisymmetric MSID of interstellar gas medium embedded with a coplanar azimuthal magnetic field. We search for both aligned and unaligned stationary configurations in a

two-dimensional self-gravitating MSID with a flat rotation curve.

Our model analysis here will give various stationary morphologies in a magnetized gas disk, including bars and lopsided, barred, and normal spiral structures. Moreover, we provide phase relationships of spatial patterns among magnetic field, gas density, and velocity perturbations that can be examined observationally. Regarding the recent wavelet analysis on multi-wavelength data of the spiral galaxy NGC 6946 (Frick et al. 2000, 2001) that revealed an extension of the interlaced magnetic and optical spiral structures into the outer disk with a largely flat rotation curve, our analysis here conveys an important message that stationary logarithmic spiral patterns of slow MHD density waves (SMDWs; Fan & Lou 1996; Lou & Fan 1998a), with interlaced spiral enhancements of magnetic field and gas density, can indeed persist in an extended MSID with a flat rotation curve (Lou & Fan 2002).

Conceptually, the stationary pattern problem here is closely tied to the density wave problem in a differentially rotating disk (Syer & Tremaine 1996; Shu et al. 2000). It is the balance between relevant wave pattern speeds and disk rotation that leads to possible nonaxisymmetric patterns stationary in an inertial frame of reference. Historically, the seminal idea of MHD density waves was contemporary (Lynden-Bell 1966; Roberts & Yuan 1970) with the early development of density wave theory four decades ago (Lin & Shu 1964, 1966; Goldreich & Lynden-Bell 1965; Toomre 1969, 1977; Lin 1967, 1987; Shu 1970a, b). While the stellar disk provides a massive"template", MHD density wave processes in the ISM disk (Fan & Lou 1996, 1997, 1999; Lou & Fan 1997, 1998a, b, 2000a, b, 2002; Lou, Han, & Fan 1999; LYF 2001; LYFL 2001) do have additional dynamic freedoms.

Theoretically, there exist complemetary perspectives, different motivations, and independent approaches to study various bar phenomena in rotating self-gravitating fluid bodies. The masterpiece of Chandrasekhar (1969) on ellipsoidal figures of equilibrium summarizes the beautiful mathematical descriptions of Maclaurin, Jacobi, Dedekind, Riemann ellipsoids and Poincaré pear-shaped configurations as well as their close interrelations on the basis of instability analyses and characteristics of bifurcations in incompressible self-gravitating fluids. Complementary numerical studies of compressible, self-gravitating, differentially rotating, nonspherical equilibrium figures have shown striking family resemblances to these classical exactly solved problems (Ostriker 1978). By collapsing the dimension along the rotation axis, one can study equilibria and stability properties of two-dimensional Riemann disks of uniform rotation relevant to central parts of disk galaxies (Weinberg & Tremaine 1983; Weinberg 1983). Another broad class of disk problems involves stability properties of singular isothermal disks (SIDs) (Zang 1976; Toomre 1977; Lemos et al. 1991; Lynden-Bell & Lemos 1993; Goodman & Evans 1999). Syer & Tremaine (1996) found solutions to a class of stationary nonaxisymmetric perturbation SID configurations. Shu et al. (2000) derived solutions for stationary perturbation configurations in isopedically magnetized SIDs and interpreted them as onsets of bar-type and barred-spiral instabilities (Galli et al. 2001). Our analysis here parallels that of Shu et al. (2000) but with a coplanar magnetic field in an MSID, and we examine the MSID problem from the perspective of stationary fast and slow MHD density waves (FMDWs and SMDWs; Fan & Lou 1996; Lou & Fan 1998a; LYF 2001). We derive a form of magnetic virial theorem for an MSID and suggest the ratio of rotation energy to the sum of gravitational and magnetic energies to be crucial for the MSID stability.

Shu et al. (2000) pursued the analogies of bar-type instabilities known in thin self-gravitating disks (Hohl 1971; Miller et al. 1970) as well as in rotating self-gravitating spheroids and ellipsoids of uniform density (Chandrasekhar 1969; Ostriker 1978) for equilibria and instabilities of isopedically magnetized SIDs. In spite of the known difficulties (Galli et al. 2001), the fascinating scenario of the so-called "fission theory" by Poincaré (1885), Liapunov (1905), and Jeans (1928) that regards incompressible ellipsoidal figures of equilibrium as potential candidates for fissioning through pear-shaped equilibria into binary stars has lead Shu et al. (2000) to speculate that nonaxisymmetric, magnetized, compressible, and perhaps truncated SIDs might prove to be promising candidates for fragmentation into binary- and multiple-star systems. They also hypothesized that a rapid loss of magnetic flux at a certain stage might hold the crucial key of resolving or bypassing the relevant known difficulties. In line with these speculations, the present MSID problem should be relevant to star formation research as well.

Based on theoretical analyses (Lau & Bertin 1978; Lin & Lau 1979; Bertin & Mark 1979) to retain higher-order effects for the WKBJ expansion of the Poisson equation, Bertin et al. (1989a, b) heuristically argued and invoked the cubic dispersion relation of density waves in a thin fluid stellar disk as the conceptual basis for classifying barred and normal spiral galaxies (viz., the Hubble classification scheme of galaxies; e.g., Lin & Lau 1979) constructed numerically by solving the standard linear integro-differential density wave equations with chosen boundary conditions. Important aspects of this modal perspective have been comprehensively summarized in Bertin & Lin (1996). In their scenario, bars and barred spirals are essentially viewed as density-wave phenomena that are better described when the effects of long-range self-gravity and differential rotation are more fully included. Specifically, the cubic dispersion relation becomes cubic in the radial wavenumber k by including the tangential shear force (TSF) for nonaxisymmetric coplanar perturbations (LYF 2001). Besides the familiar short- and long-wave branches (both are somewhat modified by the TSF), there is now a third wave branch of "open modes" characterized by even smaller k that bear striking resemblances to bars and barred spirals when superposed with an axisymmetric bulge (see Fig. 14 of Bertin et al. 1989a; Lin 1996 private communications). As we will solve the Poisson integral exactly, it would be natural to pursue the correspondence between the

modal perspective of Bertin & Lin (1996) and the (M)SID results here as well as of Shu et al.

This paper is structured as follows. We formulate in §2 the problems of full and partial MSIDs and display relevant MHD equations. Solutions and analyses for aligned and unaligned MSID configurations are presented in §3. In §4, we examine the spatial phase relationships between enhancements of gas density, magnetic field, and velocity disturbances. In §5, we discuss the connection between the modal formalism and the MSID perspective for classifying normal and barred spiral galaxies, indicate the implication to multiband observations of spiral galaxy NGC 6946, and summarize the results. Mathematical formulae are collected in Appendices A−E for the convenience of reference.

2 FORMULATION OF THE MSID PROBLEM

The key difference of our formulation and that of Shu et al. (2000) is that their magnetic field is poloidal threading across the disk and may be effectively relegated into two dimensionless parameters* Θ and ϵ (Schmitz 1987; Shu & Li 1997) such that $a^2 \to \Theta a^2$ and $G \to \epsilon G$ (a is the isothermal sound speed and G is the gravitational constant), whereas the non-force-free magnetic field of our model is azimuthal and coplanar with the disk. In essence, the effect of their poloidal magnetic field can be scaled away such that the analysis is equivalent to a hydrodynamic one, while the coplanar magnetic field of our model can give rise to new classes or features of stationary nonaxisymmetric MSID configurations. We refer to our model as an MSID problem, although the SID problem as formulated by Shu et al. (2000) is isopedically magnetized, and proceed to examine several specific aspects in an orderly manner.

2.1 Nonlinear unsteady MHD equations

For large-scale MHD processes, dissipative effects may be ignored as a first approximation. In cylindrical coordinates (r, θ, z), ideal time-dependent MHD equations include

$$\frac{\partial \Sigma}{\partial t} + \frac{1}{r}\frac{\partial (r\Sigma u)}{\partial r} + \frac{1}{r^2}\frac{\partial (\Sigma j)}{\partial \theta} = 0 \qquad (2.1.1)$$

for the mass conservation, where Σ is the vertically integrated mass density, u is the radial velocity, $j \equiv rv$ is the specific angular momentum in the vertical $\hat{z}$ direction and v is the azimuthal velocity in $\hat{\theta}-$direction,

$$\frac{\partial u}{\partial t} + u\frac{\partial u}{\partial r} + \frac{j}{r^2}\frac{\partial u}{\partial \theta} - \frac{j^2}{r^3} = -\frac{1}{\Sigma}\frac{\partial \Pi}{\partial r} - \frac{\partial \phi_T}{\partial r} - \frac{1}{\Sigma}\int \frac{dz B_\theta}{4\pi r}\left[\frac{\partial (rB_\theta)}{\partial r} - \frac{\partial B_r}{\partial \theta}\right] \qquad (2.1.2)$$

for the radial momentum equation, where Π is the vertically integrated gas pressure and ϕ_T is the total gravitational potential inclusive of that from a possible dark-matter halo,

$$\frac{\partial j}{\partial t} + u\frac{\partial j}{\partial r} + \frac{j}{r^2}\frac{\partial j}{\partial \theta} = -\frac{1}{\Sigma}\frac{\partial \Pi}{\partial \theta} - \frac{\partial \phi_T}{\partial \theta} + \frac{1}{\Sigma}\int \frac{dz B_r}{4\pi}\left[\frac{\partial (rB_\theta)}{\partial r} - \frac{\partial B_r}{\partial \theta}\right] \qquad (2.1.3)$$

for the azimuthal momentum equation in $\hat{\theta}-$direction,

$$F\phi_T = -G\oint d\psi \int_0^\infty \frac{\Sigma(\zeta, \psi, t)\zeta d\zeta}{[\zeta^2 + r^2 - 2\zeta r\cos(\psi - \theta)]^{1/2}} \qquad (2.1.4)$$

for the Poisson integral equation where $F\phi_T$ is the gravitational potential from the gas disk with $0 \le F \le 1$,

$$\frac{\partial (rB_r)}{\partial r} + \frac{\partial B_\theta}{\partial \theta} = 0 \qquad (2.1.5)$$

for the divergence-free condition on $\vec{B} \equiv (B_r, B_\theta, 0)$,

$$\frac{\partial B_r}{\partial t} = \frac{1}{r}\frac{\partial}{\partial \theta}(uB_\theta - vB_r) \qquad (2.1.6)$$

for the radial magnetic field induction equation, and

$$\frac{\partial B_\theta}{\partial t} = -\frac{\partial}{\partial r}(uB_\theta - vB_r) \qquad (2.1.7)$$

for the azimuthal magnetic field induction equation. The polytropic approximation $\Pi = a^2\Sigma$ is invoked as usual where a is the isothermal sound speed.

For a static vertical balance without a vertical flow velocity v_z, the vertical force balance takes the form of

$$0 = -\int dz\frac{\partial p}{\partial z} - \int dz\rho\frac{\partial \phi}{\partial z} - \int dz\frac{\partial}{\partial z}\frac{(B_\theta^2 + B_r^2)}{8\pi}\ , \qquad (2.1.8)$$

where gas and magnetic pressures work together against the vertical gravity towards the disk at $z = 0$.

2.2 Equilibrium of an axisymmetric MSID

For an MSID geometry of axisymmetry, one solves the MHD equations with the Poisson integral (2.1.4). We presume a flat rotation curve with a background disk angular rotation speed $\Omega = aD/r$, where D is the dimensionless rotation parameter. The cases of $D > 1$ and $D < 1$ correspond then to supersonic and subsonic MSID rotations. To avoid the magnetic field winding dilemma (Lou & Fan 1998a), the background magnetic field is taken to be azimuthal about the symmetry axis with a scaling of $B_\theta = \mathcal{F}r^{-1/2}$ where $\mathcal{F}$ is a constant. The Lorentz force of this B_θ profile † is included in the MSID radial force balance. The vertically integrated gas pressure Π_0 of the background is related to the background surface mass density Σ_0 by $\Pi_0 = a^2\Sigma_0$. The epicyclic oscillation frequency κ of a flat rotation curve is defined by $\kappa^2 \equiv (2\Omega/r)d(r^2\Omega)/dr = 2\Omega^2$, and the Alfvén speed C_A in an MSID is defined by $C_A^2 \equiv \int dz B_\theta^2/(4\pi\Sigma_0)$.

The rotation speed of a disk galaxy $V_\theta \equiv \Omega r = aD \gg C_A$ due to the presence of a massive dark-matter halo (presumed to be axisymmetric here). By the equipartition argument, the thermal and magnetic energy densities are compa-

* Specifically, $\Theta \equiv (\lambda^2 + 1 + 2\eta^2)/(\lambda^2 + \eta^2)$ and $\epsilon \equiv 1 - \lambda^{-2}$ with $\lambda \equiv 2\pi G^{1/2}\Sigma/B_z =$ const. and $\eta \equiv |\vec{g}_{\|}|/(2\pi G\Sigma)$ where $|\vec{g}_{\|}|$ is the coplanar gravitational acceleration.

† B_θ scales as r^{-1} for a force-free azimuthal magnetic field.

rable with $a \sim C_A$. It then follows that $D \gg 1$ for supersonic and super-Alfvénic rotations in typical disk galaxies.

To attribute a fraction $(1-F)$ of the total gravity in the background equilibrium to an axisymmetric dark-matter halo that is unresponsive to gas disk perturbations, one may write $\partial\phi_T/\partial r = F\partial\phi_T/\partial r + (1-F)\partial\phi_T/\partial r$. The case of $F=1$ is referred to as a full (M)SID, while the case of $0 \leq F < 1$ is referred to as a partial (M)SID (Syer & Tremaine 1996; Shu et al. 2000). In reference to equations (5), (6), (21) and (27) of Syer & Tremaine (1996), their parameter f is related to F here by $f \equiv (1-F)/F$. The background rotational equilibrium of an MSID requires

$$-\frac{a^2D^2}{r} = \frac{a^2}{r} - \frac{\partial\phi_T}{\partial r} - \frac{C_A^2}{2r} \ , \tag{2.2.1}$$

where the portion of the gravitational potential associated with the gas disk satisfies $F\partial\phi_T/\partial r = 2\pi G\Sigma_0$ in the disk plane at $z=0$, as required by the Poisson equation in a razor-thin MSID. In force balance (2.2.1), the gravity and net Lorentz forces are radially inward (i.e., an outward magnetic pressure force but a stronger inward magnetic tension force), while the gas pressure and centrifugal forces are radially outward. It follows for an MSID that

$$\Sigma_0 = F[a^2(1+D^2) - C_A^2/2]/(2\pi G r) \ . \tag{2.2.2}$$

In the context of a protostellar disk, one cannot invoke a dark-matter halo and one thus deals with a full (M)SID of $F=1$. Shu et al. (2000; also Galli et al. 2001) recently performed extensive analysis on constructions of stationary nonaxisymmetric perturbation solutions from a background axisymmetric SID that is isopedically magnetized with a poloidal magnetic field. These solutions can be classified as aligned and unaligned configurations (Kalnajs 1973) that require specific values of D^2 for their very existence. These results in idealized theoretical settings are interesting and important in that these solutions, with proper interpretations, may be pertinent to configurations of bars, barred spirals, and normal spirals in a differentially rotating disk, and may bear implications to the onset of bar or bar-type instabilities that lead to formation of these possible configurations. For example, for the aligned case of nonaxisymmetric stationary perturbations (of angular variation $\exp[-im\theta]$ with an integer m) studied by Shu et al. (2000) (see their eqns [25] – [27]), one finds an unconstrained or arbitrary D^2 for $|m|=1$ (see also equation [46] of Syer & Tremaine 1996), and $D^2 = |m|/(|m|+2)$ for $|m| \geq 2$. The latter with $D^2 < 1$ implies a subsonic protostellar disk rotation.

2.3 Coplanar MHD perturbations in an MSID

From equations (2.1.1) – (2.1.7), one derives coplanar MHD perturbation equations in an MSID of gas,

$$\frac{\partial\Sigma_1}{\partial t} + \frac{1}{r}\frac{\partial(r\Sigma_0 u_1)}{\partial r} + \Omega\frac{\partial\Sigma_1}{\partial\theta} + \frac{\Sigma_0}{r^2}\frac{\partial j_1}{\partial\theta} = 0 \ , \tag{2.3.1}$$

$$\frac{\partial u_1}{\partial t} + \Omega\frac{\partial u_1}{\partial\theta} - \frac{2\Omega j_1}{r} = -\frac{\partial}{\partial r}\left(\frac{a^2\Sigma_1}{\Sigma_0} + \phi_1\right) + \frac{C_A^2\Sigma_1}{2\Sigma_0 r} - \frac{1}{\Sigma_0}\int\frac{dzB_\theta}{4\pi r}\left[\frac{\partial(rb_\theta)}{\partial r} - \frac{\partial b_r}{\partial\theta}\right] - \frac{1}{\Sigma_0}\int\frac{dzb_\theta}{4\pi r}\frac{\partial(rB_\theta)}{\partial r} \ , \tag{2.3.2}$$

$$\frac{\partial j_1}{\partial t} + \frac{r\kappa^2}{2\Omega}u_1 + \Omega\frac{\partial j_1}{\partial\theta} = -\frac{\partial}{\partial\theta}\left(\frac{a^2\Sigma_1}{\Sigma_0} + \phi_1\right) + \frac{1}{\Sigma_0}\int\frac{dzb_r}{4\pi}\frac{\partial(rB_\theta)}{\partial r} \ , \tag{2.3.3}$$

$$\phi_1 = -G\oint d\psi\int_0^\infty\frac{\Sigma_1(\zeta,\psi,t)\zeta d\zeta}{[\zeta^2+r^2-2\zeta r\cos(\psi-\theta)]^{1/2}} \ , \tag{2.3.4}$$

$$\frac{\partial(rb_r)}{\partial r} + \frac{\partial b_\theta}{\partial\theta} = 0 \ , \tag{2.3.5}$$

$$\frac{\partial b_r}{\partial t} = \frac{1}{r}\frac{\partial}{\partial\theta}(u_1 B_\theta - r\Omega b_r) \ , \tag{2.3.6}$$

$$\frac{\partial b_\theta}{\partial t} = -\frac{\partial}{\partial r}(u_1 B_\theta - r\Omega b_r) \ , \tag{2.3.7}$$

where $\vec{b} \equiv (b_r, b_\theta, 0)$ is the coplanar magnetic field perturbation, ϕ_1 is the perturbation of $F\phi_T$ from gas distribution, and other variables with subscript $_1$ are perturbations to the pertinent equilibrium variables. Here, we set $v_z = b_z = 0$ and do not consider vertical variations across the disk. All with the harmonic $\exp(i\omega t - im\theta)$ dependence, we introduce complex radial variations $S(r)$, $U(r)$, $J(r)$, $V(r)$, $R(r)$, and $Z(r)$ for Σ_1, u_1, j_1, ϕ_1, b_r, and b_z. Coplanar MHD perturbation equations (2.3.1) – (2.3.7) can then be reduced to

$$i(\omega - m\Omega)S + \frac{1}{r}\frac{\partial}{\partial r}(r\Sigma_0 U) - \frac{im\Sigma_0}{r^2}J = 0 \ , \tag{2.3.8}$$

$$i(\omega - m\Omega)U - \frac{2\Omega J}{r} = -\frac{\partial\Phi}{\partial r} - \frac{1}{\Sigma_0}\int\frac{dzZ}{4\pi r}\frac{\partial(rB_\theta)}{\partial r} + \frac{C_A^2 S}{2\Sigma_0 r} - \frac{1}{\Sigma_0}\int\frac{dzB_\theta}{4\pi r}\left[\frac{\partial(rZ)}{\partial r} + imR\right] \ , \tag{2.3.9}$$

where $\Phi \equiv a^2 S/\Sigma_0 + V$,

$$i(\omega - m\Omega)J + \frac{r\kappa^2}{2\Omega}U = im\Phi + \frac{1}{\Sigma_0}\int\frac{dzR}{4\pi}\frac{\partial(rB_\theta)}{\partial r} \ , \tag{2.3.10}$$

$$V(r) = -G\oint d\chi\int_0^\infty\frac{S(\zeta)\cos(m\chi)\zeta d\zeta}{[\zeta^2+r^2-2\zeta r\cos\chi]^{1/2}} \ , \tag{2.3.11}$$

$$\frac{\partial(rR)}{\partial r} - imZ = 0 \ , \tag{2.3.12}$$

$$i(\omega - m\Omega)R + \frac{imB_\theta}{r}U = 0 \ , \tag{2.3.13}$$

$$i\omega Z = \frac{\partial}{\partial r}(r\Omega R) - \frac{\partial}{\partial r}(B_\theta U) \ . \tag{2.3.14}$$

It suffices to use only two of the three equations (2.3.12) – (2.3.14) for magnetic field perturbation $\vec{b} = (b_r, b_\theta, 0)$.

Rearrangement of equations (2.3.8) – (2.3.14) in terms of S, V, J and iU further leads to

$$Z = -\frac{i}{m}\frac{\partial(rR)}{\partial r} \tag{2.3.15}$$

from the divergence-free condition (2.3.12) of $\vec{b}$, and

$$R = -\frac{mB_\theta U}{r(\omega - m\Omega)} \tag{2.3.16}$$

from the radial magnetic induction equation (2.3.13). Using equations (2.3.15) and (2.3.16) in the radial and azimuthal momentum equations (2.3.9) and (2.3.10), one derives

$$\begin{aligned} i(\omega - m\Omega)U - \frac{2\Omega J}{r} &= -\frac{\partial \Phi}{\partial r} + \frac{C_A^2 S}{2\Sigma_0 r} \\ &-iC_A^2 \left[\!\!\left[\frac{1}{r^{1/2}}\frac{\partial}{\partial r}\left\{ r\frac{\partial}{\partial r}\left[\frac{U}{r^{1/2}(\omega - m\Omega)} \right] \right\} \right.\right. \\ &\left.\left. -\frac{m^2 U}{r^2(\omega - m\Omega)} + \frac{1}{2r^{1/2}}\frac{\partial}{\partial r}\left[\frac{U}{r^{1/2}(\omega - m\Omega)} \right] \right]\!\!\right] \end{aligned} \tag{2.3.17}$$

and

$$i(\omega - m\Omega)J + \frac{r\kappa^2}{2\Omega}U = im\Phi - \frac{mC_A^2 U}{2r(\omega - m\Omega)} \ . \tag{2.3.18}$$

2.4 Stationary MHD perturbations in an MSID

For nonaxisymmetric MHD perturbations stationary in an inertial frame of reference, we set $\omega = 0$ in equations (2.3.8), (2.3.16) – (2.3.18) and obtain

$$m\Omega S + \frac{1}{r}\frac{\partial}{\partial r}(r\Sigma_0 iU) + \frac{m\Sigma_0}{r^2}J = 0 \ , \tag{2.4.1}$$

$$\begin{aligned} m\Omega iU + \frac{2\Omega J}{r} &= \frac{\partial \Phi}{\partial r} - \frac{C_A^2 S}{2\Sigma_0 r} - \frac{C_A^2}{2r^{1/2}}\frac{\partial}{\partial r}\left(\frac{iU}{m\Omega r^{1/2}} \right) \\ &-\frac{C_A^2}{r^{1/2}}\frac{\partial}{\partial r}\left[r\frac{\partial}{\partial r}\left(\frac{iU}{m\Omega r^{1/2}} \right) \right] + \frac{C_A^2 miU}{\Omega r^2} \ , \end{aligned} \tag{2.4.2}$$

$$m\Omega J + \frac{r\kappa^2}{2\Omega}iU = -m\Phi + \frac{C_A^2 iU}{2\Omega r} \ , \tag{2.4.3}$$

$$iR = \frac{B_\theta iU}{\Omega r} \ , \tag{2.4.4}$$

together with equations (2.3.11), (2.3.15), and the definition of Φ after equation (2.3.9). As the pattern speed $\omega_p \equiv \omega/m$ of possible MHD density waves is set to zero in an inertial frame of reference *a priori*, these equations are to be solved to determine the proper values of the dimensionless rotation parameter D. As the system may support possible FMDWs and SMDWs (Fan & Lou 1996; Lou & Fan 1998a), two proper values of D are expected.

3 SOLUTION ANALYSIS OF STATIONARY MSID CONFIGURATIONS

3.1 The case of aligned perturbations

The case of $m = 0$ should be handled with care. It would be misleading to use equations (2.4.3) and (2.4.4). One should examine equations (2.3.8)$-$(2.3.14) with $\omega = m = 0$. By setting $U = R = 0$, equations (2.3.8), (2.3.10), (2.3.12) and (2.3.14) are satisfied, and equation (2.3.13) is identically zero. There is no constraint on Z. However, by setting $Z \propto r^{-1/2}$, $S \propto r^{-1}$, $J \propto r$, $V \propto \ln r$, and $\Phi \propto$ const.$+\ln r$, remaining equations (2.3.9) and (2.3.11) can be made consistent with a rescaling of the axisymmetric background MSID.

For the nonaxisymmetric aligned case with $m \neq 0$, one takes the density-potential pair

$$rS = \text{const.} \tag{3.1.1}$$

and

$$V = -(2\pi G/|m|)rS = \text{const.} \tag{3.1.2}$$

(e.g., Shu et al. 2000; Galli et al. 2001). For a constant iU (see eq. [3.1.4] below), the mass conservation (2.4.1) requires

$$J = -\Omega r^2 S/\Sigma_0 \ , \tag{3.1.3}$$

and the azimuthal momentum equation (2.4.3) gives consistently a constant iU by

$$iU = m(\Phi - \Omega^2 r^2 S/\Sigma_0)/[C_A^2/(2\Omega r) - \Omega r] \ . \tag{3.1.4}$$

By equations (3.1.1), (3.1.2), and (2.2.2), it follows that $\Phi \equiv a^2 S/\Sigma_0 + V =$ const. and a combination of equations (3.1.3) and (2.4.2) leads to

$$\left[m\Omega r - \frac{C_A^2(m^2 - 1/2)}{m\Omega r} \right] iU - \frac{2\Omega^2 r^2 S}{\Sigma_0} + \frac{C_A^2 S}{2\Sigma_0} = 0 \ . \tag{3.1.5}$$

Substitutions of expressions (3.1.2)$-$(3.1.4) into equation (3.1.5) give the *solution condition* or *stationary dispersion relation* for aligned nonaxisymmetric MHD perturbations,

$$\begin{aligned} \frac{m^2\Omega r - C_A^2(m^2 - 1/2)/(\Omega r)}{C_A^2/(2\Omega r) - \Omega r}\left(\frac{a^2}{\Sigma_0 r} - \frac{2\pi G}{|m|} - \frac{\Omega^2 r}{\Sigma_0} \right) \\ -\frac{2\Omega^2 r}{\Sigma_0} + \frac{C_A^2}{2\Sigma_0 r} = 0 \ . \end{aligned} \tag{3.1.6}$$

For a later examination of the spatial phase relationship between b_θ and Σ_1, we further derive the following results. By equations (2.3.15) and (2.4.4), the $\theta-$component of the magnetic field perturbation is related to iU by

$$Z = -iUB_\theta/(2m\Omega r) \ . \tag{3.1.7}$$

By using expression (3.1.4) for constant iU and expression of constant Φ in equation (3.1.7), one obtains

$$Z = -\frac{B_\theta S}{2\Sigma_0}\frac{(a^2 - 2\pi G\Sigma_0 r/|m| - \Omega^2 r^2)}{(C_A^2/2 - \Omega^2 r^2)} \ . \tag{3.1.8}$$

The solution criterion (3.1.6) may then be written as

$$\frac{a^2 - 2\pi G\Sigma_0 r/|m| - \Omega^2 r^2}{C_A^2/2 - \Omega^2 r^2} = \frac{2\Omega^2 r^2 - C_A^2/2}{m^2\Omega^2 r^2 - C_A^2(m^2 - 1/2)} \ . \tag{3.1.9}$$

By equation (3.1.8), the sign of either left-hand side (LHS) or right-hand side (RHS) of equation (3.1.9) will determine the phase relation between the surface mass density perturbation S and the azimuthal magnetic field perturbation Z.

3.2 The physical nature of the solution criterion

To fully understand the nature of solution condition (3.1.6), we examine two conceptually related cases in order. The first case of $C_A^2 = 0$ is essentially the one studied by Shu et al. (2000) ($\epsilon = 1$ and $\Theta = 1$) and can be explained as purely azimuthal propagation of hydrodynamic density waves (Lin & Shu 1964, 1966). By this clue, we proceed to show that the second case of $C_A^2 \neq 0$ corresponds to two possible situations

of purely azimuthal propagations of FMDWs and SMDWs (Lou & Fan 1998a).

3.2.1 *The aligned full and partial SID cases*

We have verified with $C_A^2 = 0$ and $F = 1$ in our analysis that the results (25) − (27) of Shu et al. (2000) come out naturally, namely, either D^2 is arbitrary for $|m| = 1$ or $D^2 = |m|/(|m| + 2)$ for $|m| \geq 2$. The latter with $D^2 < 1$ corresponds to a subsonic SID rotation.

Moreover, the solution condition (3.1.6) or (3.1.9), with $C_A^2 = 0$, can be written in the informative form of

$$m^2\Omega^2 = 2\Omega^2 + m^2a^2/r^2 - 2\pi G\Sigma_0|m|/r \ . \qquad (3.2.1)$$

In reference to the well-known WKBJ dispersion relation of density waves (Lin & Shu 1964, 1966 or equation [39] of Shu et al. 2000), equation (3.2.1) can be readily obtained by replacing the radial wavenumber $|k|$ with the azimuthal wavenumber $|m|/r$ and setting $\omega = 0$ in an inertial frame of reference. This clearly describes an azimuthal propagation of hydrodynamic density waves, and a stationary pattern in the sidereal frame of reference requires specific values of D^2 for different $|m|$ values. It was pointed out by Shu et al. (2000) that perturbations of the aligned case has no radial wave propagation. We here provide a transparent physical interpretation for the aligned case of nonaxisymmetric stationary perturbations in terms of a purely azimuthal density wave propagation (retrograde relative to the disk) advected by the SID rotation such that the stationarity is sustained. As the corotation is at infinity for a stationary perturbation and $\kappa^2 = 2\Omega^2$, a solution of equation (3.2.1) appears outside the Lindblad resonances also located at infinity. Specifically, the solution is valid inside the inner Lindblad resonance (ILR) in a finite radial range. Formally, only the solution of $|m| = 1$ appears within the Lindblad resonances.

Equation (3.2.1) is quadratic in $|m|$ and the two possible values of $|m|$ should be reminiscent of the long- and short-branches of density waves in terms of the radial wavelength $2\pi/|k|$ (e.g., Binney & Tremaine 1987), even though the $m^2\Omega^2$ term on the LHS of equation (3.2.1) is now involved in determining the proper values of $|m|$. By this perspective and for a full SID with $F = 1$, one might view the two values of $|m|$ given by equation (3.2.1), namely $|m| = 1$ with an arbitrary D^2 value, and $|m| = 2D^2/(1 - D^2)$ with $|m| \geq 2$, as “long” and “short” stationary azimuthally propagating density waves. By the latter, one requires $D^2 < 1$ and in the limit of $D^2 \to 1$, the value of $|m|$ increases to infinity corresponding to extremely short azimuthal wavelengths. Perhaps, the $|m| = 2$ case is the most interesting one that mimics a stationary *barred configuration.*

For a partial SID with $0 \leq F < 1$ and $C_A^2 = 0$, criterion (3.2.1) becomes

$$m^2D^2 = 2D^2 + m^2 - |m|F(D^2 + 1) \ . \qquad (3.2.2)$$

The two values of $|m|$ are then given by

$$|m| = \frac{-F(D^2+1) \pm [F^2(D^2+1)^2 + 8D^2(D^2-1)]^{1/2}}{2(D^2-1)} \qquad (3.2.3)$$

where negative values of $|m|$ must be rejected.

To examine the solution property of (3.2.3) for $|m|$, condition (3.2.2) may be cast into the revealing form of

$$D^2 = |m|(|m| - F)/(m^2 + F|m| - 2) \ . \qquad (3.2.4)$$

For a full SID with $F = 1$ in equation (3.2.4), one would have $D^2 = |m|/(|m| + 2) < 1$ for a subsonic SID rotation. For $F = 1$ and $|m| = 1$ in equation (3.2.4), the value of D^2 is arbitrary for a nontrivial eccentric solution (Shu et al. 2000), including the case of a cold rotating disk of $a^2 = 0$ but $\Omega r = aD \neq 0$ (see discussions of Syer & Tremaine 1996 about their eq. [43]) and the case of a non-rotating disk of $D^2 = 0$ (see discussions of Syer & Tremaine 1996 about their eq. [45]). In the limit of $F = 0$, equation (3.2.4) gives

$$D^2 = m^2/(m^2 - 2) > 1 \qquad (3.2.5)$$

(see eqns. [8], [21], [25], [44] of Syer & Tremaine 1996 with their $\beta = 0$) for a supersonic SID rotation with $|m| \geq 2$, and the case of $|m| = 1$ is forbidden because $D^2 > 0$ is required.

Similarly for $0 < F < 1$, the case of $|m| = 1$ is no longer allowed for a partial SID because $D^2 = -1$ is unphysical. In this context, we note that the corollary of Syer & Tremaine (1996) after their equation (44) is inaccurate in the sense that the situation of their $\beta = 0$ (flat rotation curve) and finite $f \neq 0$ $(0 < F < 1)$ does not allow for aligned $m = 1$ perturbation solutions. There are two distinct classes of solutions for $|m|$ in general. For $|m| < F^{-1}$, one would have a supersonic SID rotation with $D^2 > 1$, while for $|m| > F^{-1}$, one would have a subsonic SID rotation with $D^2 < 1$. It is then clear that the case of $F = 1$ excludes the possibility of $D^2 > 1$, while the case of $F = 0$ excludes the possibility of $D^2 < 1$. For $0 \leq F < 1$, all solutions with $|m| \geq 2$ satisfying condition (3.2.2) appears inside the ILR.

For spiral galaxies, a partial SID model with $0 \leq F < 1$ is more relevant due to the presence of a massive dark-matter halo and there seems to be no need to worry about the $|m| = 1$ case of aligned eccentric displacements because they only exist for a full SID with $F = 1$ (Zang 1976; Toomre 1977; Shu et al. 2000). However, in star-forming clouds not involving an axisymmetric dark-matter halo, such case of $|m| = 1$ for aligned eccentric displacements might lead to alternative SID configurations of interest (Shu et al. 2000).

3.2.2 *Aligned MSID perturbation configurations*

With $C_A^2 \neq 0$, the stationary criterion (3.1.6) or (3.1.9) for the aligned case may be cast into the informative form of

$$m^4\Omega^4 - \left[2\Omega^2 + \left(\frac{C_A^2}{r^2} + \frac{a^2}{r^2} - \frac{2\pi G\Sigma_0}{|m|r}\right)m^2 - \frac{2C_A^2}{r^2}\right]m^2\Omega^2$$
$$+\frac{m^2C_A^2}{r^2}\left[\left(\frac{a^2}{r^2} - \frac{2\pi G\Sigma_0}{|m|r}\right)\left(m^2 - \frac{1}{2}\right) - \frac{C_A^2}{4r^2}\right] = 0, \quad (3.2.6)$$

which reminds us of the dispersion relation for spiral FMDWs and SMDWs (Fan & Lou 1996; Lou & Fan 1998a; LYF 2001) by simply replacing the radial wavenumber $|k|$ with the azimuthal wavenumber $|m|/r$ and by setting $\omega = 0$ in an inertial frame of reference. In the earlier derivation

of WKBJ dispersion relation for FMDWs and SMDWs, we took a force-free $B_\theta \propto r^{-1}$. The present case of $B_\theta \propto r^{-1/2}$ is not force-free and some extra terms in expression (3.2.6) are due to the additional radial and azimuthal Lorentz force terms as well as geometric effects in equations (2.3.2) and (2.3.3). Physically, the two possible D^2 values contained in equation (3.2.6) should relate to the two situations of purely azimuthal propagation of FMDWs and SMDWs (retrograde relative to the disk) such that the disk rotation renders them stationary in an inertial frame of reference.

The equivalent criteria (3.1.6), (3.1.9), and (3.2.6) may be arranged into the form of

$$\begin{aligned}&[m^2a^2D^2 - C_A^2(m^2-1/2)]\\ &\quad\times[a^2(1-D^2) - F(a^2D^2+a^2-C_A^2/2)/|m|]\\ &\qquad+(2a^2D^2 - C_A^2/2)(a^2D^2-C_A^2/2) = 0\ . \qquad (3.2.7)\end{aligned}$$

For a full MSID with $F=1$, the LHS of expression (3.2.7) can be factored into

$$\begin{aligned}&(|m|-1)\{(a^2D^2-C_A^2)(1-D^2)a^2|m|^2\\ &\quad+(a^2D^2-C_A^2)(C_A^2/2-2a^2D^2)|m|\\ &\quad-[C_A^2/2-a^2(D^2+1)]C_A^2/2\} = 0\ . \qquad (3.2.8)\end{aligned}$$

Therefore, similar to the case of perturbations in an isopedically magnetized full SID (Shu et al. 2000), the D^2 value is unconstrained for $|m|=1$. For $|m|\geq 1$, the second factor on the LHS of equation (3.2.8) may be rearranged into

$$\begin{aligned}&|m|(2+|m|)a^4D^4 - [C_A^2/2+5C_A^2|m|/2+(a^2+C_A^2)|m|^2]a^2D^2\\ &\quad+(C_A^2/2-a^2)C_A^2/2+C_A^4|m|/2+C_A^2a^2|m|^2 = 0 \qquad (3.2.9)\end{aligned}$$

with the last coefficient being positive for $|m|\geq 1$. By (3.2.9), there are two positive values of a^2D^2, namely

$$\begin{aligned}a^2D^2 = &\frac{C_A^2/2+5C_A^2|m|/2+(a^2+C_A^2)|m|^2}{2|m|(2+|m|)}\\ &\pm\Bigg\{\left[\frac{C_A^2}{2}+\frac{5C_A^2|m|}{2}+(a^2+C_A^2)|m|^2\right]^2\\ &\quad-4|m|(2+|m|)\left[\frac{C_A^2}{2}\left(\frac{C_A^2}{2}-a^2\right)\right.\\ &\quad\left.+\frac{C_A^4|m|}{2}+C_A^2a^2|m|^2\right]\Bigg\}^{1/2}[2|m|(2+|m|)]^{-1}, \qquad (3.2.10)\end{aligned}$$

where the determinant Δ is non-negative for $|m|\geq 1$ (see Appendix A or equation [D9]).

For a partial MSID with $0\leq F<1$, expression (3.2.7) may be cast into the form of

$$\begin{aligned}&(2-m^2-F|m|)a^4D^4+(\mathcal{A}-\mathcal{B}+\mathcal{C})a^2D^2\\ &\quad-(C_A^2/m^2)(m^2-1/2)\mathcal{A}+C_A^4/4 = 0\ , \qquad (3.2.11)\end{aligned}$$

where $\mathcal{A}$, $\mathcal{B}$, $\mathcal{C}$ are defined by equations (B1), (B2), (B3) in Appendix B. We emphasize that $|m|=1$ is no longer a solution with unconstrained D^2 for a partial MSID. One may solve equation (3.2.11) for two values of a^2D^2

$$a^2D^2 = (\mathcal{B}-\mathcal{A}-\mathcal{C}\pm\Delta^{1/2})/[2(2-m^2-F|m|)]\ , \qquad (3.2.12)$$

where the determinant Δ is positive for $|m|\geq 1$ (see definition [B4] in Appendix B).

For the case of $|m|=1$, criterion (3.2.7) becomes

$$(a^2D^2-C_A^2/2)(1-F)(a^2D^2+a^2-C_A^2/2) = 0\ , \quad (3.2.13)$$

where $0<F<1$. As $2\pi G r\Sigma_0 = F[a^2(1+D^2)-C_A^2/2]>0$ is a necessary requirement, the only possible solution of a^2D^2 for a partial MSID becomes $a^2D^2 = C_A^2/2$.

3.3 Onset of bar-type instabilities in MSIDs

For the disk stability problem, there exists a key parameter for both secular and dynamic bar-type instabilities, namely, the ratio of the kinetic energy of rotation $\mathcal{T}$ to the absolute value of the gravitational potential energy $\mathcal{W}$ (Ostriker & Peebles 1973; Ostriker 1978). If one regards the stationary configuration of aligned $|m|=2$ MSID as the onset of secular bar-type instabilities (Shu et al. 2000), it is then of interest to properly estimate the ratio $\mathcal{T}/|\mathcal{W}|$. For an MSID of infinite radial extent, both quantities $\mathcal{T}$ and $\mathcal{W}$ are infinite but their ratio remains finite. Starting from the radial force balance of the background magnetorotational equilibrium

$$-\Sigma_0\Omega^2 r = -d\Pi/dr - \Sigma_0\partial\phi_T/\partial r - \Sigma_0 C_A^2/(2r)\ , \quad (3.3.1)$$

we multiply equation (3.3.1) by $2\pi r^2dr$ and integrate from 0 to a radius R which is allowed to approach infinity eventually. After an integration by parts for the gas pressure term up to R, one obtains the MSID virial theorem

$$2(\mathcal{T}+\mathcal{U})+\mathcal{W}-\mathcal{M} = 2\pi R^2\Pi(R) \qquad (3.3.2)$$

within R, where by using equation (2.2.2) for Σ_0

$$\mathcal{T}\equiv\frac{1}{2}\int_0^R\Sigma_0 r^2\Omega^2 2\pi r dr = \frac{a^4D^2F}{2G}\left[1+D^2-\frac{C_A^2}{2a^2}\right]R \quad (3.3.3)$$

is the kinetic energy of the MSID rotation,

$$\mathcal{U}\equiv\int_0^R\Pi 2\pi r dr = \frac{a^2F}{G}\left[a^2(1+D^2)-\frac{C_A^2}{2}\right]R \qquad (3.3.4)$$

is the gas internal energy,

$$\mathcal{W}\equiv-\int_0^R r\frac{d\phi_T}{dr}\Sigma_0 2\pi r dr = -\frac{a^4F}{G}\left[1+D^2-\frac{C_A^2}{2a^2}\right]^2 R \quad (3.3.5)$$

is the total gravitational potential energy (if there is no matter outside R),

$$\mathcal{M}\equiv\int_0^R\frac{\int dz B_\phi^2}{8\pi}2\pi r dr = \frac{C_A^2a^2F}{2G}\left[1+D^2-\frac{C_A^2}{2a^2}\right]R \quad (3.3.6)$$

is the MSID magnetic energy within R. The usual key ratio is then

$$\mathcal{T}/|\mathcal{W}| = a^2D^2/[2(a^2+a^2D^2-C_A^2/2)]\ . \qquad (3.3.7)$$

In view of the MHD virial theorem (3.3.2) in which $\mathcal{W}<0$ by equation (3.3.5), one might suspect the quantity $\mathcal{W}-\mathcal{M}$ to play the role of $\mathcal{W}$ in the absence of coplanar magnetic field. Because

$$\mathcal{W}-\mathcal{M} = -\frac{a^2(1+D^2)F}{G}\left[a^2(1+D^2)-\frac{C_A^2}{2}\right]R<0 \quad (3.3.8)$$

for $\Sigma_0>0$, it would be suggestive of a new modified ratio

$$\mathcal{T}/|\mathcal{W}-\mathcal{M}| = D^2/[2(1+D^2)] \qquad (3.3.9)$$

to determine the instability criterion of an MSID for nonaxisymmetric aligned MHD perturbations.

3.4 The unaligned case of stationary nonaxisymmetric MSID configurations

We now consider the unaligned case for logarithmic spiral structures (Kalnajs 1973; Shu et al. 2000). Combinations of azimuthal momentum equation (2.4.3) with radial momentum equation (2.4.2) and with mass conservation (2.4.1) give

$$\begin{aligned}&\bigg\{m^2\Omega^2r^2-\kappa^2r^2+C_A^2\\&-C_A^2\bigg[m^2-\bigg(\frac{C_A^2}{2\Omega^2r^2}-\frac{3}{2}\bigg)\bigg(\frac{C_A^2}{2\Omega^2r^2}-2\bigg)\bigg]\bigg\}iU\\&=m\Omega r^2\frac{\partial\Phi}{\partial r}+2m\Omega r\Phi-\frac{m\Omega C_A^2rS}{2\Sigma_0}\\&\quad+C_A^2\bigg[r\frac{\partial}{\partial r}\bigg(\frac{m\Omega rS}{\Sigma_0}-\frac{m\Phi}{\Omega r}\bigg)\\&\quad-\bigg(\frac{C_A^2}{2\Omega^2r^2}-\frac{5}{2}\bigg)\bigg(\frac{m\Omega rS}{\Sigma_0}-\frac{m\Phi}{\Omega r}\bigg)\bigg]\qquad(3.4.1)\end{aligned}$$

and

$$\frac{m\Omega rS}{\Sigma_0}+r\frac{\partial(iU)}{\partial r}+\bigg(\frac{C_A^2}{2\Omega^2r^2}-\frac{\kappa^2}{2\Omega^2}\bigg)iU-\frac{m\Phi}{\Omega r}=0\ .\quad(3.4.2)$$

The Poisson integral (2.3.11) is a linear integral equation and has a number of complete sets of eigenfunctions, depending on the radial range of nonzero surface mass density (Snow 1952). For a radial domain of $(0,1)$, the radial part of the eigenfunctions may be Legendre polynomials (Hunter 1963) or Bessel functions (Yabushita 1966), while for a radial domain of $(0,\infty)$, one may use Bessel functions (Toomre 1963) or logarithmic spirals (Kalnajs 1965, 1971). We here study unaligned logarithmic spiral structures.

For logarithmic spirals (Kalnajs 1965, 1971) with constant pitch angles, the known potential-density pair is

$$S=sr^{-3/2+i\alpha}\quad\text{and}\quad V=vr^{-1/2+i\alpha}\ ,\qquad(3.4.3),\ (3.4.4)$$

where α is a constant parameter that characterizes the radial variation of perturbations and the two constant coefficients s and v are related by

$$v=-2\pi G\mathcal{N}_m(\alpha)s\ ,\qquad(3.4.5)$$

$$\begin{aligned}\text{with }\ &\mathcal{N}_m(\alpha)\equiv K(\alpha,m)\\&=\frac{1}{2}\frac{\Gamma[(m+1/2+i\alpha)/2]\Gamma[(m+1/2-i\alpha)/2]}{\Gamma[(m+3/2+i\alpha)/2]\Gamma[(m+3/2-i\alpha)/2]}\qquad(3.4.6)\end{aligned}$$

being the Kalnajs function (Section IV of Kalnajs 1971) and $\Gamma(...)$ being the gamma-function (Qian 1992; Appendix A of Syer & Tremaine 1996). The Kalnajs function is real and positive. Table 1 of Kalnajs (1971) contains numerical values of $K(\alpha,m)$ for different values of α and m. For large m or large α, one has $\mathcal{N}_m(\alpha)\cong(m^2+\alpha^2)^{-1/2}$ approximately. For $m=0,1,2$, the curves of $K(\alpha,m)$ versus α were displayed in Figure 1 of Shu et al. (2000). The Kalnajs function is even in m and α. With a sufficient accuracy (Shu et al. 2000), one may approximately take

$$\mathcal{N}_m(\alpha)\cong(m^2+\alpha^2+1/4)^{-1/2}\ .\qquad(3.4.7)$$

The exact recurrence or recursion relation for $\mathcal{N}_m(\alpha)$ is

$$\mathcal{N}_{m+1}(\alpha)\mathcal{N}_m(\alpha)=[(m+1/2)^2+\alpha^2]^{-1}\qquad(3.4.8)$$

(Kalnajs 1971). Suppose one takes, for example,

$$\mathcal{N}_2(\alpha)\cong(4+\alpha^2+1/4)^{-1/2}$$

by approximation (3.4.7) with $|m|=2$, it then follows successively from the recursion (3.4.8) that

$$\mathcal{N}_1(\alpha)\cong=(1+1/16+\alpha^2/4)^{1/2}/(1+1/8+\alpha^2/2)\ <\ 1$$

and

$$\mathcal{N}_0(\alpha)\cong\frac{(1+1/8+\alpha^2/2)}{(\alpha^2+1/4)(1+1/16+\alpha^2/4)^{1/2}}$$

(see Fig. 1 of Shu et al. 2000). To achieve a higher accuracy for $\mathcal{N}_m(\alpha)$, one starts from approximation (3.4.7) with a large $|m|$ and use the recursion (3.4.8) to successively derive $\mathcal{N}_m(\alpha)$ of descending $|m|$.

Consistent with the logarithmic spiral forms of $S(r)$ and $V(r)$ by equations (3.4.3) and (3.4.4), we take U to be

$$iU=iur^{-1/2+i\alpha}\ ,\qquad(3.4.9)$$

where u is a constant coefficient. It follows from equations (2.4.1), (2.4.2), (3.4.5), (2.3.12), and (2.3.15) that

$$\frac{m\Omega s}{\Sigma_0}+iu\bigg(i\alpha+\frac{C_A^2}{2\Omega^2r^2}-\frac{3}{2}\bigg)-\frac{m}{\Omega r}\bigg(\frac{a^2s}{r\Sigma_0}+v\bigg)=0\ ,\quad(3.4.10)$$

$$\begin{aligned}&\bigg\{m^2\Omega^2r^2-\kappa^2r^2-C_A^2\bigg[m^2-1\\&\quad-\bigg(\frac{C_A^2}{2\Omega^2r^2}-\frac{3}{2}\bigg)\bigg(\frac{C_A^2}{2\Omega^2r^2}-2\bigg)\bigg]\bigg\}iu\\&=C_A^2\bigg(i\alpha+2-\frac{C_A^2}{2\Omega^2r^2}\bigg)\bigg[\frac{m\Omega s}{\Sigma_0}-\frac{m}{\Omega r}\bigg(\frac{a^2s}{r\Sigma_0}+v\bigg)\bigg]\\&\quad+m\Omega r(i\alpha+3/2)\bigg(\frac{a^2s}{r\Sigma_0}+v\bigg)-\frac{m\Omega C_A^2s}{2\Sigma_0}\ ,\qquad(3.4.11)\end{aligned}$$

$$iR=\frac{r^{1/2}B_\theta}{\Omega r}iur^{-1+i\alpha}=\frac{B_\theta iU}{\Omega r}\ ,\qquad(3.4.12)$$

$$Z=-\frac{i\alpha r^{1/2}B_\theta}{m\Omega r}iur^{-1+i\alpha}=-\frac{i\alpha B_\theta}{m\Omega r}iU\ .\qquad(3.4.13)$$

Equation (3.4.10) relates s and iu by relation (3.4.5). Independently, equation (3.4.11) is another relation for s and iu by relation (3.4.5). A combination of the two resulting relations in terms of s and iu then gives rise to the solution criterion for stationary logarithmic spirals in an MSID. With an exact cancellation of the imaginary part, the *solution criterion* or *dispersion relation* for stationary unaligned logarithmic spirals becomes

$$\begin{aligned}&\bigg(\frac{a^2s}{r\Sigma_0}+v\bigg)\bigg[\frac{3}{2}\bigg(\frac{C_A^2}{2\Omega^2r^2}-\frac{3}{2}\bigg)-\alpha^2\bigg]-\frac{C_A^2s}{2\Sigma_0r}\bigg(\frac{C_A^2}{2\Omega^2r^2}-\frac{3}{2}\bigg)\\&=\bigg[m\Omega r-\frac{2\Omega r}{m}-C_A^2\bigg(\frac{\alpha^2-1}{m\Omega r}+\frac{m}{\Omega r}\bigg)\bigg]\\&\quad\times\bigg[\frac{m}{\Omega r}\bigg(\frac{a^2s}{r\Sigma_0}+v\bigg)-\frac{m\Omega s}{\Sigma_0}\bigg]\qquad(3.4.14)\end{aligned}$$

where s and v are related by equation (3.4.5). A physically more revealing form of criterion (3.4.14) is

$$\begin{aligned}&m^4\Omega^4-\{2\Omega^2+[C_A^2/r^2+a^2/r^2-2\pi G\mathcal{N}_m(\alpha)\Sigma_0/r]\\&\quad\times(m^2+\alpha^2+1/4)-2C_A^2/r^2\}m^2\Omega^2\end{aligned}$$

$$+(m^2C_A^2/r^2)\{[a^2/r^2-2\pi G\mathcal{N}_m(\alpha)\Sigma_0/r]$$
$$\times(m^2+\alpha^2+1/4-1/2)-C_A^2/(4r^2)\}=0\ . \qquad (3.4.15)$$

In parallel, the two stationary solution criteria (3.2.6) and (3.4.15) for the *aligned* and *unaligned* cases correspond to each other remarkably well, especially in view of the effective wavenumber $(m^2+\alpha^2+1/4)^{1/2}r^{-1}$ (Shu et al. 2000). Again, the form of equation (3.4.15) reminds us of the dispersion relation for spiral FMDWs and SMDWs (Lou 1996; Fan & Lou 1996; Lou & Fan 1998a; LYF 2001). These logarithmic spiral MHD density waves propagate in both radial and azimuthal directions relative to the MSID. For stationary logarithmic spirals in an inertial frame of reference, criterion (3.4.15) leads to two possible values of a^2D^2. As both $\kappa^2\equiv 2\Omega^2$ and Σ_0 contain the D^2 parameter, the determination of D^2 should be somewhat different from the standard WKBJ wave results derived in a background that is prescribed *a priori*. For example, for a full SID that is isopedically magnetized, Shu et al. (2000) obtains only one real solution of α at a given D^2 for each $m\geq 1$ as shown in their Fig. 3 instead of the two branches of long- and short-waves (see also Syer & Tremaine 1996 for a discussion). While for a sufficiently large D^2 value in the special case of $m=0$, there are two values of α as shown in their Fig. 2, bordering the ring fragmentation regime.

Equation (3.4.15) may be cast into the form of

$$[a^2-\Omega^2r^2-2\pi G\mathcal{N}_m(\alpha)\Sigma_0 r]$$
$$\times[(m^2+\alpha^2+1/4)\Omega^2r^2-(m^2+\alpha^2-1/4)C_A^2]$$
$$=-\alpha^2\Omega^4r^4-(C_A^2/2-3\Omega^2r^2/2)^2\ . \qquad (3.4.16)$$

After a straightforward rearrangement using the Σ_0 profile (2.2.2), criterion (3.4.16) becomes

$$[m^2+\alpha^2+1/4-(m^2+\alpha^2-1/4)C_A^2/(a^2D^2)]$$
$$\times\{a^2-[(1+D^2)a^2-C_A^2/2]F\mathcal{N}_m(\alpha)\}$$
$$-a^2D^2[m^2-2-(m^2+\alpha^2-1)C_A^2/(a^2D^2)]$$
$$+(C_A^2/2)[C_A^2/(2a^2D^2)-3/2]=0\ . \qquad (3.4.17)$$

For $C_A^2=0$ and $F=1$, this criterion reduces to equation (37) of Shu et al. (2000). Also with $C_A^2=0$ and $\alpha^2\to 0$ in the so-called "breathing mode" regime, one obtains

$$m^2D^2=2D^2+(m^2+1/4)[1-(1+D^2)F\mathcal{N}_m(0)]\ , \quad (3.4.18)$$

which differs from condition (3.2.2) derived earlier for the aligned case, especially in the regime of large $|m|$.

In terms of a quadratic algebraic equation for a^2D^2, equation (3.4.17) may be written in the explicit form of

$$[m^2-2+(m^2+\alpha^2+1/4)F\mathcal{N}_m(\alpha)]a^4D^4 \qquad (3.4.19)$$
$$-(\mathcal{A}+\mathcal{B}+\mathcal{C})a^2D^2+\frac{C_A^2(m^2+\alpha^2-1/4)\mathcal{A}}{(m^2+\alpha^2+1/4)}-\frac{C_A^4}{4}=0\ ,$$

where $\mathcal{A}$, $\mathcal{B}$, $\mathcal{C}$ are defined by equations $(C1)$, $(C2)$, $(C3)$ in Appendix C. For $|m|\geq 2$ in equation (3.4.19), the coefficient of a^4D^4 is positive, the coefficient of a^2D^2 is negative, and the remaining coefficient is positive. By the definition of $\mathcal{N}_1(\alpha)$, this statement remains valid with $|m|=1$ for the first two coefficients and for the last coefficient with an *additional sufficient* requirement $a^2>C_A^2/4$. The determinant Δ of the quadratic equation (3.4.19) is positive for $|m|\geq 2$ such that there are two positive a^2D^2 (see Appendix C).

One can further show, in a similar manner, that the determinant Δ of equation (3.4.19) is non-negative for $F=1$ and $|m|=1$ with *sufficient* requirements $\alpha\geq\sqrt{3}/2$ and $a\geq C_A/2$. In other words, there are two positive values of D^2 as long as $\alpha\geq\sqrt{3}/2$ and $a\geq C_A/2$.

For $F=1$, $m=0$, and a α greater than a specific value α_c in equation (3.4.19), one can show that the coefficient of a^4D^4 is positive, the coefficient of a^2D^2 is negative, and the remaining coefficient is positive. Following the same procedure of proof, one can further show that there exist two positive roots of a^2D^2. For $0\leq\alpha\leq\alpha_c$, however, the solution structure of condition (3.4.19) may have several possiblities, depending on the ratio $q^2\equiv C_A^2/a^2$. In terms of q^2, α, and $\mathcal{N}_0(\alpha)$, the two solutions of D^2 are

$$D^2=\Bigg[\!\!\Bigg[\{[1-(1-q^2/2)\mathcal{N}_0(\alpha)](\alpha^2+1/4)+q^2(\alpha^2-1/4)\mathcal{N}_0(\alpha)+q^2(\alpha^2-7/4)\}$$
$$\pm\Big[\{[1-(1-q^2/2)\mathcal{N}_0(\alpha)](\alpha^2+1/4)+q^2(\alpha^2-1/4)\mathcal{N}_0(\alpha)+q^2(\alpha^2-7/4)\}^2$$
$$-4[-2+(\alpha^2+1/4)\mathcal{N}_0(\alpha)]\{q^2(\alpha^2-1/4)\times[1-(1-q^2/2)\mathcal{N}_0(\alpha)]-q^4/4\}\Big]^{1/2}\Bigg]\!\!\Bigg]$$
$$\times\{2[-2+(\alpha^2+1/4)\mathcal{N}_0(\alpha)]\}^{-1}\ , \qquad (3.4.20)$$

where the denominator changes from negative to positive between $\alpha\sim 1.79$ and 1.795 approximately[‡]; this value of α, independent of q^2, is denoted by α_c. We shall refer to the two values of D^2 as the plus- and minus-sign solutions according to their respective signs in front of the square root of the determinant in equation (3.4.20). As specific examples, we explored numerically three cases with decreasing values of ratio q^2, namely, (a) $q^2=3.61$ (Fig. 1a), (b) $q^2=1.0$ (Fig. 1b), and (c) $q^2=0.09$ (Fig. 1c). For $\alpha>\alpha_c$, there are indeed two positive values of D^2 as stated earlier. The larger and smaller ones correspond to the plus- and minus-sign solutions, respectively. As $\alpha\to\alpha_c+0^+$, the plus-sign solution goes to $+\infty$, while the minus-sign solution remains finite and continuous across α_c. For $q^2\neq 0$, there exists a finite interval $\alpha_l<\alpha<\alpha_u$ such that the determinant Δ is *negative* and there are thus no real solutions for D^2. Approximately, α_l is between 0.595 and 0.6 while α_u is between 0.815 and 0.82 for $q^2=3.61$; α_l is between 0.68 and 0.685 while α_u is between 0.92 and 0.925 for $q^2=1.0$; and α_l is between 0.96 and 0.965 while α_u is between 1.08 and 1.085 for $q^2=0.09$. There is a systematic shift of this open interval (α_l,α_u) towards larger α as q^2 decreases. For $\alpha_u\leq\alpha\leq\alpha_c$,

[‡] We used an approximate expression of $\mathcal{N}_0(\alpha)$. Shu et al. (2000) derived a value of $|\alpha_c|=1.759$ from the same condition $(\alpha_c^2+1/4)\mathcal{N}_0(\alpha_c)=2$.

the plus-sign solution is negative while the minus-sign solution changes from negative to positive for increasing α. For $0 \le \alpha \le \alpha_l$, the minus-sign solution is greater than the plus-sign solution and the two solutions join at $\alpha = \alpha_l$ with a $D^2 > 0$; for $q^2 = 1$ and $q^2 = 0.09$, the smaller plus-sign solutions change from negative to positive as α increases from $\alpha = 0$ within this interval. All negative values of D^2 are not shown in Fig. 1 as they are unphysical.

There are now two ring fragmentation regimes when α is sufficiently large (one for larger D^2 and one for smaller D^2) and one modified collapse regime for sufficiently small α and D^2 as shown in Figure 1 for all three q^2 values. In the limit of $q^2 \to 0$, the situation degenerates to the case shown in Figure 2 of Shu et al. (2000) as expected (see also Lemos et al. 1991 on the linear stability of axisymmetric scale-free disks to axisymmetric disturbances). For increasing values of q^2, the lower ring fragmentation regime associated with slow MHD disturbances is enlarged while the upper ring fragmentation regime associated with fast MHD disturbances is pushed upwards in the parameter scheme of Fig. 1. That is, one needs an even larger D^2 to access the upper ring fragmentation regime.

As the MHD generalization of Toomre's Q-parameter, the Q_M-parameter (Lou & Fan 1998a) is defined by

$$Q_M \equiv \frac{(a^2+C_A^2)^{1/2}\kappa}{\pi G\Sigma_0} = \frac{2\sqrt{2}D(1+q^2)^{1/2}}{F(1+D^2-q^2/2)} \qquad (3.4.21)$$

with an MSID profile (2.2.2). For axisymmetric FMDWs, the disk stability requires $Q_M > 1$ (Lou & Fan 1998a). For the minima D^2_{min} of the boundaries of the upper fragmentation regime and the relevant values of q^2, the corresponding values of Q_M thus obtained are fairly close to unity in all three cases of Figure 1. For example, with $q^2 = 3.61$, $D^2_{min} = 40.62$ at $\alpha = 3.9$ and $Q_M = 0.972$; with $q^2 = 1.0$, $D^2_{min} = 15.24$ at $\alpha = 3.681$ and $Q_M = 0.992$; and with $q^2 = 0.09$, $D^2_{min} = 6.48$ at $\alpha = 3.264$ and $Q_M = 1.01$. It appears that the critical Q_M value tends to increase slightly with decreasing values of q^2 and with decreasing values of critical α. This trend is also complemented by the limiting case (Shu et al. 2000) with $q^2 = 0$, $D^2_{min} = 5.41$ at $\alpha = 3.056$, and $Q_M = 1.026$. Thus the approximate instability criterion $Q_M \lesssim 1$ (Fan & Lou 1996; Lou & Fan 1998a) appears pertinent to the upper branch of ring fragmentation for axisymmetric fast MHD disturbances (see Fig. 1).

Comparing with Fig. 2 of Shu et al. (2000), the coplanar magnetic field modifies the collapse regime as shown in our Fig. 1 and introduces the lower regime of ring fragmentation for slow MHD disturbances when α is sufficiently large. These instabilities do not occur when D^2 is large: $D^2 \gtrsim 9.2$ for $q^2 = 3.61$; $D^2 \gtrsim 3.5$ for $q^2 = 1$; $D^2 \gtrsim 1.2$ for $q^2 = 0.09$; and $D^2 \gtrsim 0.932$ for $q^2 = 0$. The last result of $q^2 = 0$ is taken from subsection 4.1 of Shu et al. (2000).

From equation (3.4.13) and

$$iU = \left(\frac{m\Phi}{\Omega r} - \frac{m\Omega rS}{\Sigma_0}\right)\left(i\alpha + \frac{C_A^2}{2\Omega^2 r^2} - \frac{3}{2}\right)^{-1}, \qquad (3.4.22)$$

we derive

$$Z = -\frac{i\alpha B_\theta S}{\Omega^2 r}\left[\frac{a^2}{r\Sigma_0} - 2\pi G\mathcal{N}_m(\alpha) - \frac{\Omega^2 r}{\Sigma_0}\right] \times\left(i\alpha + \frac{C_A^2}{2\Omega^2 r^2} - \frac{3}{2}\right)^{-1}, \qquad (3.4.23)$$

which is important to determine the spatial phase relationship between the surface mass density and azimuthal magnetic field perturbations. In the limit of $\alpha \to 0$, one has $Z \to 0$, but iU given by (3.4.22) remains nonzero. For a small $\alpha \neq 0$ such that α^2 may be dropped relative to $i\alpha$ term, Z and S are phase shifted by $\sim \pm\pi/2$.

In the limit of $\alpha \to \infty$, we obtain

$$Z = -\frac{B_\theta S}{\Sigma_0\Omega^2 r^2}[a^2 - 2\pi G\mathcal{N}_m(\alpha)\Sigma_0 r - \Omega^2 r^2] \qquad (3.4.24)$$

which, given stationary condition (3.4.16), can be cast into a convenient form to examine the spatial phase relationship between Z and S in an MSID plane at $z = 0$.

4 PHASE RELATIONSHIPS BETWEEN MAGNETIC FIELD AND MASS DENSITY

We examine spatial phase relationships among velocity disturbances, azimuthal magnetic field, and surface mass density enhancements because they provide useful observational diagnostics for magnetized spiral galaxies (Beck & Hoernes 1996; Fan & Lou 1996; Lou & Fan 1998a, 2002; Frick et al. 2000). Regions of high-density gas are vulnerable to active star formation, while nonthermal radio-continuum emissions from gyrating relativistic cosmic-ray electrons trapped in a spiral galaxy would reveal regions of stronger magnetic field. Thus, large-scale spiral structures of optical and radio-continuum emissions contain valuable information of the underlying MHD (Lou & Fan 2000a, b). The mathematical development is somewhat lengthy and the relevant formulae are summarized in Appendices D and E for aligned and unaligned perturbations respectively. A reader may want to mainly concentrate on the flow of logics with convenient references to equations in the two Appendices.

4.1 Aligned MSID Configurations

For a full MSID of $F = 1$, D^2 as given by solution (3.2.10) depends only on two dimensionless parameters $q^2 \equiv C_A^2/a^2$ and $|m|$. By solutions (3.2.10), one derives equation $(D1)$ that shows $a^2D^2 - C_A^2/2 > 0$ for the upper *plus-sign* solution in equation $(D1)$. For the lower *minus-sign* solution in equation $(D1)$, whether inequality $a^2 > C_A^2|m|/[2(|m|-1)]$ holds or not in the determinant Δ would determine whether $a^2D^2 - C_A^2/2 > 0$ or not.

By equation $(D1)$, we then examine the sign of $2\pi G\Sigma_0 r = F(a^2 + a^2D^2 - C_A^2/2)$ for a full MSID of $F = 1$. An addition of a^2 to the first term on the RHS of equation $(D1)$ gives equation $(D2)$. Examine then the determinant Δ in solutions (3.2.10) or $(D1)$ in the form of equation $(D3)$. The sum of the last two terms in expression $(D3)$ is given

by expression ($D4$). When $a^2 > C_A^2/4$, we have the background surface mass density $\Sigma_0 > 0$ for both the plus- and minus-sign solutions (3.2.10) of a^2D^2. For $a^2 < C_A^2/4$, one has $\Sigma_0 > 0$ for the plus-sign solution only; the minus-sign solution gives $\Sigma_0 < 0$ which is unphysical.

To examine the spatial phase relationship between b_θ and Σ_1 in the MSID plane, we use relations (3.1.8) and (3.1.9) derived in subsection 3.1. Specifically, we determine the signs of both numerator and denominator on the RHS of equation (3.1.9). For the numerator $2\Omega^2r^2 - C_A^2/2 = 2(a^2D^2 - C_A^2/2 + C_A^2/4)$, we add $C_A^2/4$ to the first term on the RHS of equation ($D1$) to derive equation ($D5$). The determinant Δ may be cast into the form of equation ($D6$). For $a^2 - C_A^2/4 > 0$ in equation ($D6$), one has both $\Sigma_0 > 0$ and $2a^2D^2 - C_A^2/2 > 0$ for either plus- or minus-solutions in equation (3.2.10). For $a^2 - C_A^2/4 < 0$, only the plus-sign solution with $a^2D^2 - C_A^2/4 > 0$ is physically valid.

For the sign of the denominator on the RHS of equation (3.1.9) as given by equation ($D7$), a subtraction of $C_A^2 - C_A^2/(2m^2)$ from the first term on the RHS of solution (3.2.10) leads to expression ($D8$). We now examine the determinant Δ in the form of expression ($D9$). The last term containing $(3|m|^2 - 2)$ on the RHS of equation ($D9$) is positive for $|m| \neq 0$. Hence, the denominator $m^2\Omega^2r^2 - C_A^2(m^2-1/2)$ is positive and negative for the plus- and minus-sign solutions in equation (3.2.10), respectively.

To examine the sign of the background surface mass density Σ_0 of a partial MSID for $|m| \geq 1$, we consider $a^2D^2 + a^2 - C_A^2/2$. By adding $a^2 - C_A^2/2$ to the term involving $\mathcal{B} - \mathcal{A} - \mathcal{C}$ on the RHS of solution (3.2.12) for a^2D^2, one has inequality ($D10$). In the determinant Δ of solution (3.2.12), we then consider the part as given by equation ($D11$). When $a^2 - C_A^2/4 > 0$, Σ_0 is positive for solutions (3.2.12) of both signs; for $a^2 - C_A^2/4 < 0$, Σ_0 is positive for the plus-sign solution, while $\Sigma_0 < 0$ for the minus-sign solution. These conclusions for a partial MSID ($0 \leq F < 1$) turn out exactly the same as those for a full MSID ($F = 1$).

To examine the phase relationship between Z and S, equations (3.1.7)$-$(3.1.9) remain valid with Σ_0 profile (2.2.2) for a partial MSID. Again, we examine the signs of the numerator and denominator on the RHS of (3.1.9). For the numerator, we consider $a^2D^2 - C_A^2/4$ by subtracting $C_A^2/4$ from the term involving $\mathcal{B} - \mathcal{A} - \mathcal{C}$ on the RHS of solution (3.2.12) for a^2D^2. The resulting expression is then given by equation ($D12$). In the determinant Δ of solution (3.2.12), we then consider the part given by equation ($D13$). Therefore, Σ_0 and $a^2D^2 - C_A^2/4$ are positive for both plus- and minus-sign solutions of (3.2.12) when $a^2 - C_A^2/4 > 0$. For $a^2 - C_A^2/4 < 0$, only the plus-sign solution is valid with $a^2D^2 - C_A^2/4 > 0$; the minus-sign gives a $D^2 < 0$.

We now examine the sign of the denominator on the RHS of equation (3.1.9). For this purpose, we consider $a^2D^2 - [1 - 1/(2m^2)]C_A^2$. In the determinant Δ of solution (3.2.12), we consider the portion given by equation ($D14$), which vanishes for $|m| = 1$ and is positive for $|m| \geq 2$. Thus, $m^2\Omega^2r^2 - C_A^2(m^2 - 1/2)$ is positive and negative for the plus- and minus-sign solutions of (3.2.12), respectively. Using these results in equations (3.1.8) and (3.1.9), we have Z and S being out of phase for the plus-sign solution of (3.2.12), and Z and S being in phase for the minus-sign solution of (3.2.12) when $a^2 > C_A^2/4$. When $a^2 < C_A^2/4$, the minus-sign solution of (3.2.12) leads to a negative Σ_0.

Based on these analyses and in reference to equations (3.1.8) and (3.1.9) for the phase relationships between Z and S, perturbation enhancements of b_θ and Σ_1 anticorrelate and correlate with each other for the plus- and minus-sign solutions, respectively, when $a^2 > C_A^2/4$. When $a^2 < C_A^2/4$, the minus-sign solution is invalid because the surface mass density Σ_0 would be negative. These two distinct stationary aligned MSID configurations appear as results of differential rotation, self-gravity, and curved magnetic field. According to equation (3.1.4), one may write

$$iU = \frac{m\Omega rS}{\Sigma_0}\frac{(a^2 - 2\pi G\Sigma_0 r/|m| - \Omega^2r^2)}{(C_A^2/2 - \Omega^2r^2)} \ . \tag{4.1.1}$$

Therefore, $iU \propto \pm rS$, $iR \propto \pm rS$, and $J \propto -S$ for the plus- and minus-sign solutions. With these spatial phase relationships among stationary perturbation variables, one may conceive mental pictures for the two distinct types of stationary MSID bar configurations for $|m| = 2$. For the plus-sign case, enhancements of b_θ and Σ_1 are out of phase with each other. High-density gas regions are active in star formation (i.e., bright in optical and infrared bands) with enhanced small-scale random magnetic fields (i.e., bright in total nonthermal radio-continuum emissions), whereas relatively strong regular magnetic field regions should be bright in polarized radio-continuum emissions with higher degrees of polarization (less disturbed by activities associated with cloud and star formation on small scales). For the minus-sign case, enhancements of b_θ and Σ_1 are in phase. By the same rationale, the structural manifestations of bars or lopsided disks in *total* and *polarized* radio emissions will be in competition because small-scale random motions tend to enhance total radio-continuum emissions while weaken polarized radio-continuum emissions. Regions of strong total radio-continuum, optical, infrared emissions should more or less overlap. Depending on the level of activities in star-forming regions, polarized radio-continuum emissions may also be sufficiently strong in optically bright regions. Polarized radio-continuum emissions from relatively weak magnetic field regions should show higher degrees of polarization because of reduced level star formation activities there.

4.2 Unaligned Logarithmic MSID Spirals

We first consider the important factor that appears in criterion (3.4.16) for logarithmic spirals in an MSID, as given by equation ($E1$). By equations (3.4.16) and (3.4.23), the sign of this factor ($E1$) determines the spatial phase relationship between b_θ and Σ_1. Using the stationary criterion in the form of equation (3.4.19), we derive two values of a^2D^2 as given by equation ($E2$). The determinant Δ under the square root of solution ($E2$) can be shown to be non-negative for $|m| \geq 2$ (see Appendix C). As $\Omega^2r^2 = a^2D^2$, we

subtract $C_A^2\{1-[2(m^2+\alpha^2+1/4)]^{-1}\}$ from solution ($E2$) and rearrange the determinant Δ of solution ($E2$) accordingly. In the expression of determinant Δ, we consider the relevant part as given by equation ($E3$), which is positive for $|m|\geq 2$. For a full MSID of $F=1$ with $|m|=1$ and $|m|=0$, the reader is referred to numerical results and discussions that follow equation (3.4.19). It then follows with $|m|\geq 2$ that the key factor ($E1$) (see solution criterion [3.4.16]), namely $(m^2+\alpha^2+1/4)\Omega^2 r^2-(m^2+\alpha^2-1/4)C_A^2$, is positive and negative for *plus-* and *minus-sign* solutions of a^2D^2 in equation ($E2$), respectively.

Using dispersion relation (3.4.16) for stationary logarithmic spirals in an MSID and relation (3.4.23) between Z and S derived in subsection 3.4, we finally arrive at

$$Z\propto \pm S\{\alpha^2+i\alpha[C_A^2/(2\Omega^2 r^2)-3/2]\} \qquad (4.2.1)$$

for the plus- and minus-sign solutions of a^2D^2 in equation ($E2$), respectively. For a sufficiently large α in the tight-winding or WKBJ regime, one may ignore the imaginary part in relation (4.2.1). In this regime, Z is approximately in-phase and out-of-phase with S for the plus- and minus-sign solutions, respectively. This appears to be consistent with the results of FMDW and SMDW analyses in the tight-winding approximation (Fan & Lou 1996; Lou & Fan 1998a, 2002). For a sufficiently small α that corresponds to relatively open spiral structures, we may drop the α^2 term in comparison with the term proportional to $i\alpha$. In this regime of small $\alpha\neq 0$, Z is either ahead of or lag behind S by a phase difference of $\sim\pi/2$ for both stationary fast and slow logarithmic spiral configurations in an MSID; this is a new result, not known before.

5 DISCUSSION AND APPLICATIONS

5.1 A discussion on bars and barred spirals

The modal formulation and computations of Bertin et al. (1989a, b) and Bertin & Lin (1996) set a theoretical framework to classify morphologies of spiral galaxies. Meanwhile, the analytical and numerical results of Shu et al. (2000; also Galli et al. 2001) provide an important perspective for the onsets of bar-type and barred-spiral instabilities in isopedically magnetized SIDs associated with nonaxisymmetric aligned disturbances and unaligned logarithmic spiral perturbations that appear stationary in an inertial frame of reference. One would like to know the overall connection between the results and interpretations of Shu et al. (2000) and those of Bertin et al. (1989a, b; Bertin & Lin 1996), especially regarding the cubic dispersion relation and accurately solved numerical solutions in the modal scenario for bars and barred spiral galaxies. Among several apparent differences in the model formulations such as SIDs versus prescribed disks, logarithmic spiral perturbations versus normal modes, stationarity versus time variations, exact analytical solutions versus extended WKBJ approximation as well as accurate numerical solutions, we single out one key element that, we believe, distinguishes the two independent lines of approach in a significant manner. The issue involves analyses that are somewhat technical and subtle. We shall describe them below.

For SIDs and their kin (Mestel 1963), there have been theoretical studies on their structures and instability properties for decades (Zang 1976; Toomre 1977; Lemos et al. 1991; Lynden-Bell & Lemos 1993; Syer & Tremaine 1996; Evans & Read 1998; Goodman & Evans 1999; Shu et al. 2000; Galli et al. 2001) in view of their potential applications to the structure of lopsided or normal and barred spiral galaxies, to the light cusps seen in the nuclei of galaxies, and to the formation and collapse of cloud cores in the birth of stars and planetary systems. Syer & Tremaine (1996) found semianalytic and numerical solutions of nonaxisymmetric stationary equilibria for completely flattened (razor-thin) power-law disks. The basic problem along with pertinent issues have been well summarized by Shu et al. (2000), and for the special case of index $\beta=0$ (in the notation of Syre & Tremaine 1996), Shu et al. (2000) derived analytic solutions and criteria for both aligned and unaligned logarithmic stationary perturbations in razor-thin isopedically magnetized SIDs.

For aligned perturbations, the zero-frequency solutions correspond to the onset of bifurcations from axisymmetric SIDs to nonaxisymmetric SIDs in close analogy to bifurcations from incompressible uniformly rotating Maclaurin spheroids to Dedekind ellipsoids with configuration axes that remain fixed in space (Chandrasekhar 1969; Binney & Tremaine 1987). Moreover, Shu et al. (2000) relate the aligned case of $m=2$ to the onset of the secular barlike instability in the context of galactic dynamics (Hohl 1971; Miller et al. 1970; Kalnajs 1972; Ostriker & Peebles 1973; Bardeen 1975; Aoki et al. 1979; Vandervoort 1982, 1983).

In analyses of Feldman & Lin (1973), Lau & Bertin (1978), Lin & Lau (1979) and Bertin et al. (1989a, b) on galactic density waves, there is a coefficient, usually referred to as B, in the standard integro-differential equations for spiral density waves, namely

$$B=-\frac{m^2}{r^2}-\frac{4m\Omega(d\nu/dr)}{\kappa r(1-\nu^2)}+\frac{2m\Omega}{r^2\kappa\nu}\frac{d\ln[\kappa^2/(\mu_\circ\Omega)]}{d\ln r} \qquad (5.1)$$

(see eq. [25b] of Lin & Lau 1979 or eq. [2.5] of Bertin et al. 1989b), where $\nu^2\equiv(\omega-m\Omega)^2/\kappa^2$. The third term on the RHS of equation (5.1) is related to the corotation resonance and the second term on the RHS of (5.1) contains the information of the T_1 or J^2 term proportional to $d\ln\Omega/d\ln r$ with $J^2\equiv(2\pi G\mu_\circ/\kappa^2)^2T_1$ (Lau & Bertin 1978; Bertin et al. 1989b; cf. comments of Hunter 1983, Lou & Fan 1998b, and MYE 1999). The second term on the RHS of (5.1) may be split further into the form of

$$-\frac{4m\Omega(d\nu/dr)}{\kappa r(1-\nu^2)}=\frac{4m^2\Omega^2}{\kappa^2r^2(1-\nu^2)}\frac{d\ln\Omega}{d\ln r}+\frac{4m\Omega\nu}{\kappa^2r(1-\nu^2)}\frac{d\kappa}{dr}\ , \qquad (5.2)$$

where the first item on the RHS is the $-T_1/(1-\nu^2)$ term (the notation T_1 was introduced by Lau & Bertin [1978]), or equivalently, $-J^2/(1-\nu^2)$ term (the notation J^2 was later used by Lin & Lau [1979] and Bertin et al. [1989a, b]; see footnote 2 of Lou & Fan 1998b). To derive the cubic disper-

sion relation of density waves, this T_1 or J^2 term plays the central role (Bertin et al, 1989b; Bertin & Lin 1996). The second term of the RHS of equation (5.2) has been somehow ignored and relegated to a residual R term (see equation [B18] in Appendix B of Lau & Bertin 1978). Without this J^2 parameter, the cubic dispersion relation simply reduces to the quadratic one in the radial wavenumber k for spiral density waves. In short, it is this T_1 or J^2 term that is responsible for the third small k root of the so-called "open mode" besides the familiar long- and short-waves (see eq. [3.1] of Bertin et al. 1989b). In our discussion here, this J^2 mechanism is referred to as the TSF effect by its physical nature (LYF 2001).

The utmost reason we pinpoint this B coefficient is as follows. Bertin et al. (1989a, b) and Bertin & Lin (1996) proposed the cubic dispersion relation that was derived by keeping some higher-order terms in the expansion of the Poisson equation. In proper parameter regimes, two of the k roots correspond to the familiar short- and long-branches of spiral density waves while in others, there exists a third small k solution that was referred to as the "open mode" and was suggested to correspond to barred spiral galaxies on the basis of their extensive numerical calculations for the integro-differential equations of density waves (Bertin et al. 1989a, b; Bertin & Lin 1996). In contrast, Shu et al. (2000) studied the two cases of aligned and unaligned non-axisymmetric stationary perturbations in isopedically magnetized razor-thin SIDs and derived the marginal criteria for both cases. Shu et al. (2000) suggested that the class of aligned stationary perturbations is related to the secular barlike instability in galactic dynamics. This type of barlike ($m = 2$) instability may be suppressed by introducing a sufficiently massive dark-matter halo (Ostriker & Peebles 1973). By numerically studying time-dependent overreflection process of spiral waves across the corotation radius, Shu et al. (2000) further recommended that the marginal criterion for unaligned logarithmic stationary perturbations as an indicator for the onset of spiral instabilities in the sense that they be eventually amplified by a swing process near corotation (Goldreich & Lynden-Bell 1965; Mark 1976; Fan & Lou 1997). By comparing their marginal criterion (38) with their standard WKBJ dispersion relation (39) for spiral density waves (Lin & Shu 1966, 1968) and by identifying an effective wavenumber $(m^2 + \alpha^2 + 1/4)^{1/2} r^{-1}$ as defined by their equation (40), an analogy of quadratic (*rather than cubic*) form in the effective wavenumber is apparent. Shu et al. (2000) proposed to use their marginal criterion (38) in the limit of $\alpha \to 0$ (i.e., "breathing mode" limit; Lemos et al. 1991) for the onset of dynamical barred-spiral instability. The question now is the connection or relation between the two seemingly different proposals for the same physical problem in the galactic context, namely the nature of *galactic bars and barred spiral galaxies*.

The key is to realize the following basic fact. For the very SID model (9) as prescribed by Shu et al. (2000), the third corotation resonance term on the RHS of B expression (5.1) vanishes.[§] For their SID model (9), the second term on the RHS of equation (5.1) becomes

$$-\frac{4m\Omega(d\nu/dr)}{\kappa r(1-\nu^2)} = -\frac{4m\Omega\omega}{\kappa^2 r^2(1-\nu^2)} \tag{5.3}$$

which vanishes for $\omega = 0$. Remarkably, a recombination of the two terms on the RHS of equation (5.2) makes the $-T_1$ term or J^2 term needed for the cubic dispersion relation (Bertin et al. 1989b) *disappear*. In reference to equation (5.1) and the stationarity requirement (i.e., $\omega = 0$), it turns out that $B = -m^2/r^2$. Physically, this means that the TSF is absent for stationary logarithmic spiral perturbations in the SID model (9) as given by Shu et al. (2000) and should be the reason that in the analysis of Shu et al. (2000), there is no obvious clue or counterpart for the "open mode" as a root of a cubic dispersion relation. In fact, equation (38) of Shu et al. (2000) together with their approximate expression (36) for the Kalnajs function give a striking quadratic form in terms of their effective wavenumber.

It seems plausible that the "open mode" might correspond to the "aligned" SID case (Shu 2000, private communications). It is then the absence of the TSF for stationary logarithmic spiral perturbations in SIDs that decouples the "aligned" and "unaligned" cases. In other words, the nonzero TSF for time-dependent normal mode perturbations in differentially rotating disks other than SIDs might somehow couple or mingle the aligned and unaligned cases such that some kind of dispersion relation in the spirit of a cubic dispersion relation emerges. Although radial propagation is absent for aligned nonaxisymmetric perturbations in a SID, there is an azimuthal wave propagation relative to the axisymmetric background SID as made clear in our analysis. Once present, the TSF might play a nontrivial coupling role for nonaxisymmetric MSID perturbations. A carefully designed numerical test may be needed to settle this issue.

We also note another line of reasoning. Even though equation (38) of Shu et al. (2000) is approximately *quadratic* in terms of their effective wavenumber $k = \alpha_e \tilde{\omega}^{-1}$ with $|\alpha_e| \equiv (m^2 + \alpha^2 + 1/4)^{1/2}$, the recommended marginal criterion (37) (equivalently, eqs. [38] or [41]) for unaligned stationary logarithmic spiral perturbations yields only one solution of α for a given D^2 and $m \neq 0$ in a full SID (see Figure 3 of Shu et al. 2000). In other words, by setting D^2 equal to a (sufficiently large, $D^2 > 0.5368$) constant in Figure 3 of Shu et al. (2000), there is only one intersection for a given $m \neq 0$ and the corresponding root of α for a stationary logarithmic spiral may be either large or small depending upon whether D^2 is large or small. The point here is that the situation of only one root of α for stationary logarithmic spirals with $m \neq 0$ in a full SID does not necessarily contradict the familiar result of short and long spiral density waves (the two roots for the radial wavenumber k) for propagating WKBJ spiral patterns in disks that are not full SIDs (e.g., in

[§] We could not identify the B_s term attributed to Lin & Lau (1979) by Shu et al. (2000) in the paragraph following their equation (53) (i.e. the last paragraph of their subsection 5.1).

partial SIDs). By the same argument, the quadratic form of the marginal criterion in terms of the effective wavenumber $\alpha_e \tilde{\omega}^{-1}$ for stationary logarithmic spirals in SIDs might not necessarily contradict the cubic dispersion relation (Bertin et al. 1989; Bertin & Lin 1996) for nonstationary WKBJ-type spiral waves in disks that are not full SIDs.

5.2 Implications for the spiral galaxy NGC 6946

The unambiguous case of interlaced optical and magnetic spiral arms in the nearby spiral galaxy NGC 6946 was first reported by Beck & Hoernes (1996) in the almost rigidly rotating inner disk portion. Similar interlaced arm features were also suspected earlier in portions of spiral galaxies IC 342 (Krause et al. 1989) and M83 (NGC 5236; Sukumar & Allen 1989). These earlier observations, the one of NGC 6946 in particular, prompted Fan & Lou (1996) to propose the concepts of FMDWs and SMDWs in magnetized spiral galaxies (Lou & Fan 1998a; LYF 2001). Specifically, spiral perturbation enhancements of magnetic field and gas mass density of SMDWs are significantly phase shifted relative to each other (with a phase difference $\gtrsim \pi/2$). As high-density gas arms are more vulnerable to cloud and star formation activities and large-scale regular magnetic fields are less disturbed by small-scale ISM turbulence associated with star formation processes along phase-shifted magnetic arms, this scenario naturally leads to interlaced optical and magnetic spiral structures in magnetized disk galaxies. The recent wavelet analysis on multi-wavelength data of NGC 6946 (Frick et al. 2000, 2001) revealed extended spiral arms well into the outer disk portion with a flat rotation curve (e.g., Tacconi & Young 1989; Sofue 1996; Ferguson et al. 1998), which might appear to challenge our earlier proposal that SMDWs be largely confined within the inner disk portion of almost rigid rotation.

Given the idealizations in our MSID model, the two possibilities of stationary logarithmic spiral fast and slow MHD perturbations (see eq. [4.2.2]) in an MSID of flat rotation curve are conceptually important for magnetized barred or normal spiral galaxies in general (Lou & Fan 2002) and may bear direct import to the multi-wavelength data analysis on NGC 6946 by Frick et al. (2000). In particular, for stationary slow MHD logarithmic spirals in an MSID with flat rotation curve, spiral enhancements of magnetic field and mass density are interlaced with a phase difference $\gtrsim \pi/2$ by relation (4.2.1). For large α in the WKBJ regime, this phase difference approaches $\sim \pi$, while for small $\alpha \neq 0$ in the open regime, this phase difference approaches $\sim \pi/2$. Our analytical solutions include the effects of long-range self-gravity and disk differential rotation. Therefore in magnetized spiral galaxies, slow MSID patterns can indeed give rise to radially extended manifestations of interlaced optical and magnetic spiral structures that persist well into the outer disk portion with a largely flat rotation curve (Lou & Fan (2002).

We also note by equation (4.2.1) that for stationary fast logarithmic spiral structures in a full or partial MSID with a flat rotation curve, spiral enhancements of magnetic field and mass density are in phase in the tight-winding regime but are interlaced by a phase difference of $\sim \pi/2$ in the open regime. This is a new feature that may bear consequences for observations of galactic structures.

5.3 Summary

In reference to the work of Shu et al. (2000) on stationary perturbation configurations of isopedically magnetized SID, we have investigated both full and partial MSID stationary perturbation configurations with a magnetic field coplanar with the disk plane. Given the model specifications, we have reached the following conclusions and suggestions.

(1) For the aligned case with $a^2 > C_A^2/4$, there are two possible values for the rotation parameter D corresponding to purely azimuthal propagations of FMDWs and SMDWs, respectively, with distinctly different spatial phase relationships between azimuthal magnetic field and surface mass density enhancements; when $a^2 < C_A^2/4$, there is only one valid value of D^2. Also, the case of $m = 0$ can be made to correspond to a rescaling of the axisymmetric MSID background. Eccentric $|m| = 1$ displacements may occur for unconstrained D^2 values in a full MSID. In the aligned case of barred configurations with $m = 2$, there are two different possible types of phase relationships between magnetic field and mass density that should be worthwhile to search for observationally.

(2) For a partial SID with a flat rotation curve, stationary eccentric $|m| = 1$ displacements are not allowed. For a partial MSID with a flat rotation curve, stationary eccentric $|m| = 1$ displacements can no longer occur for arbitrary D^2; they may appear only when $a^2 D^2 = C_A^2/2$. For disk galaxies, it is the usual case that $\Omega^2 r^2 = a^2 D^2 > C_A^2$ due to the presence of massive dark-matter halos. One needs other physical conditions to produce stationary eccentric $|m| = 1$ displacements in disk galaxies (e.g., power-law rotation curves with $\beta \neq 0$; see Fig. 5 of Syer & Tremaine 1996).

(3) For the unaligned logarithmic spiral case, there are two values of D^2 for $|m| \geq 2$ corresponding to FMDWs and SMDWs with distinct spatial pattern relationships between azimuthal magnetic field and mass density enhancements. For $m = 0$, there are now two ring fragmentation regimes and one modified collapse regime as shown in Fig. 1. In the absence of a coplanar magnetic field, the small-D^2 ring fragmentation regime disappears. In terms of phase relationships between azimuthal magnetic field and surface mass density enhancements, the results in full and partial MSIDs are basically the same. That is, in the tight-winding regime, the two enhancements are in phase for fast MSID configurations but are out of phase for slow MSID configurations. For open structures, the two enhancements are phase shifted by $\sim \pi/2$ for either fast and slow MSID configurations.

(4) The MSID virial theorem (3.3.2) is suggestive that the modified ratio $\mathcal{T}/|\mathcal{W} - \mathcal{M}| = D^2/[2(1 + D^2)]$ be crucial to determine the stability property of an MSID with a coplanar azimuthal magnetic field, where $\mathcal{T} > 0$ is the rotational kinetic energy, $\mathcal{W} < 0$ is the gravitational potential

energy, and $\mathcal{M} > 0$ is the magnetic energy of the entire MSID system.

(5) Regarding the conceptual connection between the cubic dispersion relation in the modal formulation (Bertin et al. 1989a, b; Bertin & Lin 1996) and the perspective of stationary SID configurations (Shu et al. 2000), we suggest that the absence of the tangential shear force (TSF) in a SID of a flat rotation curve decouples the bar modes (i.e., aligned configurations) from the spiral modes (i.e., unaligned logarithmic spiral configurations). This property is also carried over to our investigation of stationary MSID configurations with a coplanar magnetic field.

(6) While our model formulation is idealized, the results provide a conceptual basis and useful clues for diagnostics of galactic bars and lopsided or barred and normal magnetized spiral galaxies. For example, for stationary unaligned logarithmic spiral patterns of SMDWs, the interlaced optical and radio-continuum spiral structures may well extend into the disk domain with a largely flat rotation curve as in the case of NGC 6946 (Lou & Fan 2002).

ACKNOWLEDGMENTS

I thank F. H. Shu for valuable discussions. This research was supported in part by grants from US NSF (ATM-9320357 and AST-9731623) to the University of Chicago, by the ASCI Center for Astrophysical Thermonuclear Flashes at the University of Chicago under Department of Energy contract B341495, by the Visiting Scientist Program of the National Science Council (NSC-88-2816-M-001-0010-6 and NSC89-2816-M001-0006-6) at the Institute of Astronomy and Astrophysics, Academia Sinica, by the Special Funds for Major State Basic Science Research Projects of China, and by the Collaborative Research Fund from the National Natural Science Foundation of China (NSFC) for Young Overseas Chinese Scholars (NSFC 10028306) at the National Astronomical Observatory, Chinese Academy of Sciences. Institutional affiliations share this contribution.

6 APPENDIX A

The proof of determinant $\Delta > 0$ in equation (3.2.10) goes as follows. Before factorization (3.2.8) we solve equation (3.2.7) with $F = 1$ for two values of a^2D^2 as

$$a^2D^2 = (\mathcal{B} - \mathcal{A} - \mathcal{C} \pm \Delta^{1/2})/[2(2 - m^2 - |m|)] \ , \qquad (A1)$$

where

$$\mathcal{A} \equiv m^2[a^2 - a^2/|m| + C_A^2/(2|m|)] > 0 \ , \qquad (A2)$$

$$\mathcal{B} \equiv 3C_A^2/2 > 0 \ , \qquad (A3)$$

$$\mathcal{C} \equiv C_A^2(m^2 - 1/2)(1 + 1/|m|) > 0 \ , \qquad (A4)$$

and the determinant Δ

$$\Delta = (\mathcal{A} + \mathcal{B} - \mathcal{C})^2 + C_A^4(m^2 + |m| - 2) + 2C_A^2(1 - 2/m^2)\mathcal{A} \geq 0 \qquad (A5)$$

for $|m| \geq 1$. In solution $(A1)$ for a^2D^2, one can factor out $(|m| - 1)$ based on the following three factorizations,

$$[1 - 1/(2m^2)]\mathcal{A} - C_A^2/4 = (|m| - 1)[(|m| + 1)\mathcal{A}/m^2 + (a^2 - C_A^2/2)/(2|m|)] \ , \qquad (A6)$$

$$2(2 - |m|^2 - |m|) = -2(|m| - 1)(|m| + 2) \ , \qquad (A7)$$

$$\mathcal{A} - \mathcal{B} + \mathcal{C} = (|m| - 1)[|m|a^2 + C_A^2/2 + C_A^2(|m| + 1)^2/|m| - C_A^2/(2|m|)] \ . \qquad (A8)$$

This then completes the proof that the determinant Δ is non-negative for $|m| \geq 1$ in solution (3.2.10) for a^2D^2.

7 APPENDIX B

As in Appendix A, we introduce handy notations

$$\mathcal{A} \equiv m^2[a^2 - a^2F/|m| + C_A^2F/(2|m|)] > 0 \ , \qquad (B1)$$

$$\mathcal{B} \equiv 3C_A^2/2 > 0 \ , \qquad (B2)$$

$$\mathcal{C} \equiv C_A^2(m^2 - 1/2)(1 + F/|m|) > 0 \ . \qquad (B3)$$

The determinant Δ in solution (3.2.12) may be written as

$$\Delta = (\mathcal{A} + \mathcal{B} - \mathcal{C})^2 + C_A^4(m^2 + F|m| - 2) + 2C_A^2(1 - 2/m^2)\mathcal{A} > 0 \qquad (B4)$$

for $|m| \geq 1$. Both solutions of a^2D^2 in (3.2.12) are positive.

8 APPENDIX C

Parallel to the proofs given in Appendices A and B, we outline the proof here by introducing a set of handy notations

$$\mathcal{A} \equiv [a^2 - (a^2 - C_A^2/2)F\mathcal{N}_m(\alpha)](m^2 + \alpha^2 + 1/4) \ , \qquad (C1)$$

$$\mathcal{B} \equiv C_A^2(m^2 + \alpha^2 - 1/4)F\mathcal{N}_m(\alpha) \ , \qquad (C2)$$

$$\mathcal{C} \equiv C_A^2(m^2 + \alpha^2 - 7/4) \ . \qquad (C3)$$

The determinant Δ of equation (3.4.19) is given by

$$\Delta \equiv (\mathcal{A} + \mathcal{B} + \mathcal{C})^2 - 4[m^2 - 2 + (m^2 + \alpha^2 + 1/4)F\mathcal{N}_m(\alpha)] \times [C_A^2(m^2 + \alpha^2 - 1/4)\mathcal{A}/(m^2 + \alpha^2 + 1/4) - C_A^4/4] > 0 \quad (C4)$$

for $|m| \geq 2$. One needs to shuffle and regroup a few terms by noting a $-4\mathcal{AB}$ term and adding $2\mathcal{C}(\mathcal{A} - \mathcal{B})$ and $-2\mathcal{C}(\mathcal{A} - \mathcal{B})$ terms and so forth. It is useful to refer to Figure 1 of Shu et al. (2000) for the magnitudes of $\mathcal{N}_m(\alpha)$ $(m = 0, 1, 2)$.

9 APPENDIX D

For aligned perturbation configurations constructed from a full MSID of $F = 1$, D^2 as given by equation (3.2.10) depends on $q^2 \equiv C_A^2/a^2$ and $|m|$. By solutions (3.2.10),

$$a^2D^2 - C_A^2/2 = [(|m| + 1)C_A^2/2 + a^2|m|^2]/[2|m|(2 + |m|)] \pm [2|m|(2 + |m|)]^{-1}\{[C_A^2(|m| + 1)/2 + a^2|m|^2]^2 - 2C_A^2|m|(2 + |m|)(|m| + 1)[a^2(|m| - 1) - C_A^2|m|/2]\}^{1/2} \qquad (D1)$$

An addition of a^2 to the first term on the RHS of solution ($D1$) gives

$$[(|m|+1)C_A^2/2+a^2|m|^2]/[2|m|(2+|m|)]+a^2$$
$$=[(|m|+1)C_A^2/2+3a^2|m|^2+4a^2|m|]/[2|m|(2+|m|)]\ . \quad (D2)$$

Examine then the determinant Δ in solutions (3.2.10) or ($D1$) in the form of

$$[(|m|+1)C_A^2/2+3a^2|m|^2+4a^2|m|]^2$$
$$-4a^2(m^2+2|m|)(|m|+1)(2a^2|m|+C_A^2/2)$$
$$-2C_A^2|m|(2+|m|)(|m|+1)[a^2(|m|-1)-C_A^2|m|/2]\ . \quad (D3)$$

The sum of the last two terms of expression ($D3$) is

$$-8(|m|^2+2|m|)(|m|+1)|m|(a^2-C_A^2/4)(a^2+C_A^2/2)\ . \quad (D4)$$

When $a^2>C_A^2/4$, the background surface mass density $\Sigma_0>0$ for both the plus- and minus-sign solutions (3.2.10) of a^2D^2. For $a^2<C_A^2/4$, one has $\Sigma_0>0$ only for the plus-sign solution, while the minus-sign solution gives $\Sigma_0<0$.

For the numerator $2\Omega^2r^2-C_A^2/2=2(a^2D^2-C_A^2/2+C_A^2/4)$ on the RHS of equation (3.1.9), we add $C_A^2/4$ to the first term on the RHS of solution ($D1$) to derive

$$\frac{(|m|+1)C_A^2/2+a^2|m|^2}{2|m|(2+|m|)}+\frac{C_A^2}{4}$$
$$=\frac{(|m|^2+3|m|+1)C_A^2/2+a^2|m|^2}{2|m|(2+|m|)}>0\ . \qquad (D5)$$

The determinant Δ may be rearranged into the form of

$$\Delta=[(|m|^2+3|m|+1)C_A^2/2+a^2|m|^2]^2$$
$$-C_A^2(|m|^2+2|m|)(3|m|^2-2)(a^2-C_A^2/4)\ . \qquad (D6)$$

For $a^2-C_A^2/4>0$ in equation ($D6$), one has both $\Sigma_0>0$ and $2a^2D^2-C_A^2/2>0$ for either plus- or minus-solutions in equation (3.2.10). For $a^2-C_A^2/4<0$, only the plus-sign solution with $a^2D^2-C_A^2/4>0$ is physically valid.

The denominator on the RHS of equation (3.1.9) is

$$m^2\Omega^2r^2-C_A^2(m^2-1/2)=m^2[\Omega^2r^2-C_A^2+C_A^2/(2m^2)]\ . \quad (D7)$$

A subtraction of $C_A^2-C_A^2/(2m^2)$ from the first term on the RHS of solution (3.2.10) gives

$$\frac{C_A^2/2+5C_A^2|m|/2+(a^2+C_A^2)|m|^2}{2|m|(2+|m|)}-\left(1-\frac{1}{2m^2}\right)C_A^2$$
$$=\frac{3C_A^2(1-|m|)/2+(a^2-C_A^2)|m|^2+2C_A^2/|m|}{2|m|(2+|m|)}\ . \qquad (D8)$$

The determinant Δ is now examined in the form of

$$\Delta=[3C_A^2(1-|m|)/2+(a^2-C_A^2)|m|^2+2C_A^2/|m|]^2$$
$$+C_A^4(|m|+2)(|m|+1)(3|m|^2-2)/|m|^2>0 \qquad (D9)$$

for $m\neq 0$.

For the sign of the background surface mass density Σ_0 of a partial MSID with $|m|\geq 1$, we consider $a^2D^2+a^2-C_A^2/2$. By adding $a^2-C_A^2/2$ to the term containing $\mathcal{B}-\mathcal{A}-\mathcal{C}$ on the RHS of solution (3.2.12) for a^2D^2, one has

$$\frac{m^2a^2+2a^2(m^2+F|m|/2-2)+(|m|-|m|^{-1})C_A^2F/2}{2(m^2+F|m|-2)}>0\ . \quad (D10)$$

In the determinant Δ of solution (3.2.12), we then consider the following part

$$-2(a^2-C_A^2/2)(m^2+F|m|-2) \qquad (D11)$$
$$\times[2(a^2-C_A^2/2)(m^2+F|m|-2)+2(\mathcal{A}-\mathcal{B}+\mathcal{C})]$$
$$+4C_A^2[(m^2-1/2)\mathcal{A}/m^2-C_A^2/4](2-m^2-F|m|)$$
$$=-8(m^2+F|m|-2)(m^2-1)(a^2+C_A^2/2)(a^2-C_A^2/4)\ ,$$

where $\mathcal{A}$, $\mathcal{B}$, $\mathcal{C}$ are defined by equations ($B1$), ($B2$), ($B3$) in Appendix B. When $a^2-C_A^2/4>0$, Σ_0 is positive for solutions (3.2.12) of both signs; for $a^2-C_A^2/4<0$, Σ_0 is positive for the plus-sign solution, while $\Sigma_0<0$ for the minus-sign solution.

For the numerator on the RHS of (3.1.9), we consider $a^2D^2-C_A^2/4$ by subtracting $C_A^2/4$ from the term involving $\mathcal{B}-\mathcal{A}-\mathcal{C}$ on the RHS of solution (3.2.12) and obtain

$$\frac{a^2(m^2-|m|F)+(m^2+2|m|F-2-F/|m|)C_A^2/2}{2(m^2+F|m|-2)}>0\ . \quad (D12)$$

For the determinant Δ of solution (3.2.12), we then consider the following part

$$C_A^2(m^2+F|m|-2)[\mathcal{A}-\mathcal{B}+\mathcal{C}-C_A^2(m^2+F|m|-2)/4]$$
$$+4C_A^2[(m^2-1/2)\mathcal{A}/m^2-C_A^2/4](2-m^2-F|m|) \qquad (D13)$$
$$=-C_A^2(m^2+F|m|-2)(3m^2-2)(a^2-C_A^2/4)(1-F/|m|),$$

where $\mathcal{A}$, $\mathcal{B}$, $\mathcal{C}$ are defined in Appendix B.

For the sign of the denominator on the RHS of equation (3.1.9), we consider $a^2D^2-[1-1/(2m^2)]C_A^2$. In the determinant Δ of solution (3.2.12), we consider the portion

$$(2-1/m^2)C_A^2(m^2+F|m|-2)$$
$$\times[2(\mathcal{A}-\mathcal{B}+\mathcal{C})-(2-1/m^2)C_A^2(m^2+F|m|-2)]$$
$$+4C_A^2[(m^2-1/2)\mathcal{A}/m^2-C_A^2/4](2-m^2-F|m|)$$
$$=C_A^4(m^2+F|m|-2)(m^2-1)(3m^2-2)/m^4\ . \qquad (D14)$$

Thus, $m^2\Omega^2r^2-C_A^2(m^2-1/2)$ is positive and negative for the plus- and minus-sign solutions of (3.2.12), respectively.

10 APPENDIX E

We consider the following factor that appears in criterion (3.4.16) for logarithmic spirals in an MSID,

$$(m^2+\alpha^2+1/4)\Omega^2r^2-(m^2+\alpha^2-1/4)C_A^2 \qquad (E1)$$
$$=(m^2+\alpha^2+1/4)\left\{\Omega^2r^2-\left[1-\frac{1}{2(m^2+\alpha^2+1/4)}\right]C_A^2\right\}\ .$$

Using the stationary criterion in the form of equation (3.4.19), we derive two values of a^2D^2

$$a^2D^2=\frac{\mathcal{A}+\mathcal{B}+\mathcal{C}\pm\Delta^{1/2}}{2[m^2-2+(m^2+\alpha^2+1/4)F\mathcal{N}_m(\alpha)]}\ , \qquad (E2)$$

where $\mathcal{A}$, $\mathcal{B}$, $\mathcal{C}$, and Δ are defined by equations ($C1$)$-$($C4$) in Appendix C. The determinant Δ is non-negative for $|m|\geq 2$. We subtract $C_A^2\{1-[2(m^2+\alpha^2+1/4)]^{-1}\}$ from solution ($E2$) and rearrange the determinant Δ of solution ($E2$). In the determinant Δ, we consider the following part,

$$[m^2-2+(m^2+\alpha^2+1/4)F\mathcal{N}_m(\alpha)]$$

Figure 1. Parameter regimes in terms of D^2, α, and $q^2 \equiv C_A^2/a^2$ separated by stationary MSID configurations for unaligned logarithmic spirals with $m = 0$. (a) $q^2 = 3.61$; (b) $q^2 = 1.0$; (c) $q^2 = 0.09$.

$$
\begin{aligned}
&\times[2 - 1/(m^2 + \alpha^2 + 1/4)]C_A^2 \\
&\times\{2(\mathcal{A} + \mathcal{B} + \mathcal{C}) - [m^2 - 2 + (m^2 + \alpha^2 + 1/4)F\mathcal{N}_m(\alpha)] \\
&\times[2 - 1/(m^2 + \alpha^2 + 1/4)]C_A^2\} \\
&-4[m^2 - 2 + (m^2 + \alpha^2 + 1/4)F\mathcal{N}_m(\alpha)] \\
&\times[C_A^2(m^2 + \alpha^2 - 1/4)\mathcal{A}/(m^2 + \alpha^2 + 1/4) - C_A^4/4] \\
&\quad = C_A^4[m^2 - 2 + (m^2 + \alpha^2 + 1/4)F\mathcal{N}_m(\alpha)] \\
&\qquad \times\{[2 - 1/(m^2 + \alpha^2 + 1/4)][2(\alpha^2 + 1/4) \\
&\qquad\quad +(m^2 - 2)/(m^2 + \alpha^2 + 1/4)] + 1\} \ , \qquad (E3)
\end{aligned}
$$

which is positive for $|m| \geq 2$.

REFERENCES

Aoki S., Noguchi M., Iye M., 1979, PASJ, 31, 737
Baldwin J.E., et al., 1980, MNRAS, 193, 313
Bardeen J.M., 1975, in Dynamics of Stellar Systems, IAU Symposium No. 69, ed. Hayli A., p. 297, Reidel, Dordrecht.
Barth, A.J., et al., 1995, AJ, 110, 1009
Beck R., 2001 preprint
Beck R., Hoernes P., 1996, Nature, 379, 47
Beck R., et al., 1996, ARA&A, 34, 155
Beck, R., et al., 1999, Nature, 397, 324
Bertin G., et al., 1989a, ApJ, 338, 78
Bertin G., et al., 1989b, ApJ, 338, 104
Bertin G., Lin C.C., 1996, Spiral Structure in Galaxies: A Density Wave Theory. MIT Press, Cambridge, Mass.
Bertin G., Mark J. W.-K., 1979, SIAM J. Appl. Math., 36, 407
Binney J., Tremaine S., 1987, Galactic Dynamics. Princeton University Press, Princeton, New Jersey
Chandrasekhar S., 1960, Proc. Nat. Acad. Sci., 46, 253
Chandrasekhar S., 1961, Hydrodynamic and Hydromagnetic Stability. Dover Publications, New York
Chandrasekhar S., 1969, Ellipsoidal Figures of Equilibrium (New York: Dover)
Evans N.W., Read J.C.A., 1998, MNRAS, 300, 106
Fan Z.H., Lou Y.-Q., 1996, Nature, 383, 800
Fan Z.H., Lou Y.-Q., 1997, MNRAS, 291, 91
Fan Z.H., Lou Y.-Q., 1999, MNRAS, 307, 645
Feldman S.I., Lin C.C., 1973, Studies Appl. Math., 52, 1
Ferguson A.M.N., et al., 1998, ApJ, 506, L19
Frick P., et al. 2000, MNRAS, 318, 925
Frick P., Beck R., Berkhuijsen E.M., Patrickeyev I., 2001, preprint
Galli D., Shu F.H., Laughlin G., Lizano S., 2001, ApJ, 551, 367
Goldreich P., Lynden-Bell D., 1965, MNRAS, 130, 97
Goodman J., Evans N.W., 1999, MNRAS, 309, 599
Hohl F., 1971, ApJ, 168, 343
Hunter C., 1963, MNRAS, 126, 299
Hunter C., 1983, in Fluid Dynamics in Astrophysics and Geophysics, ed. N. R. Lebovitz (Providence, American Mathematical Society), p. 179.
Kalnajs A.J., 1965, PhD thesis, Harvard University
Kalnajs A.J., 1971, ApJ, 166, 275
Kalnajs A.J., 1972, ApJ, 175, 63
Kalnajs A.J., 1973, Proc. Astron. Soc. Australia, 2, 174
Kronberg P.P., 1994, Rep. Prog. Phys., 57, 325
Lau Y.Y., Bertin G., 1978, ApJ, 226, 508
Lau Y.Y., Mark J. W.-K., 1976, Proc. Natl. Acad. Sci., 73, 3785
Lemos J.P.S., Kalnajs A.J., Lynden-Bell D., 1991, ApJ, 375, 484
Lin C.C., 1987, Selected Papers of C.C. Lin. World Scientific, Singapore.
Lin C.C., Shu F.H., 1964, ApJ, 140, 646
Lin C.C., Shu F.H., 1966, Proc. Natl. Acad. Sci. U.S.A., 55, 229
Lin C.C., Lau Y.Y., 1979, Studies Appl. Math., 60, 97
Lin C.C., Yuan C., Shu F., 1969, 155, 721
Lou Y.-Q., 1996, MNRAS, 279, L67
Lou Y.-Q., Fan Z.H., 1997, Communications in Nonlinear Science & Numerical Simulation, 2 (No. 2), 59
Lou Y.-Q., Fan Z.H., 1998a, ApJ, 493, 102
Lou Y.-Q., Fan Z.H., 1998b, MNRAS, 297, 84
Lou Y.-Q., Han J.L., Fan Z.H., 1999, MNRAS, 308, L1
Lou Y.-Q., Fan Z.H., 2000a, MNRAS, 315, 646
Lou Y.-Q., Fan Z.H., 2000b, in *The Interstellar Medium in M31 and M33.* 232 WE-Heraeus Seminar, eds. E.M. Berkhuijsen, R. Beck, R.A.M. Walterbos (Aachen: Shaker Verlag), 205
Lou Y.-Q., Yuan C., Fan Z.H., 2001, ApJ, 552, 189 (LYF)
Lou Y.-Q., Yuan C., Fan Z.H., Leon S., 2001, ApJ, 553, L35
Lou Y.-Q., Walsh W.M., Han J.L., Fan Z.H., 2002, ApJ, 567, 289
Lou Y.Q., Fan Z.H., 2002, MNRAS, 329, L62
Lynden-Bell D., 1966, Observatory, 86, 57
Lynden-Bell, D. 1989, MNRAS, 237, 1099
Lynden-Bell D., Lemos J.P.S., 1993, astro-ph/9907093
Mark J.W.-K., 1971, ApJ, 169, 455
Mark J.W.-K., 1976, ApJ, 205, 363
Mestel L., 1963, MNRAS, 126, 553
Miller R.H., Prendergast K.H., Quirk W.J., 1970, ApJ, 161, 903
Ostriker J.P. 1978, in *Theoretical Principles in Astrophysics and Relativity*, ed. N. R. Lebovitz, W. H. Reid, and P. O. Vandervoort (Chicago: University of Chicago Press), pp. 59-68.
Ostriker J.P., Peebles P.J.E., 1973, ApJ, 186, 467
Parker E.N., 1966, ApJ, 145, 811
Qian E., 1992, MNRAS, 257, 581
Richter O.-G., Sancisi R., 1994, A&A, 290, L9
Rix H.-W., Zaritsky D., 1995, ApJ, 447, 82
Roberts W.W., Jr., Yuan C., 1970, ApJ, 161, 887
Schmitz F., 1987, A&A, 179, 167
Shu F.H. 1970a, ApJ, 160, 89
Shu F.H. 1970b, ApJ, 160, 99
Shu F.H., Li Z.-Y. 1997, ApJ, 475, 251
Shu F.H., Laughlin G., Lizano S., Galli D., ApJ, 2000, 535, 190
Snow C., 1952, Hypergeometric and Legendre Functions with Applications to Integral Equations of Potential Theory (NBS, AMS-19) (Washington: National Bureau of Standards).
Sofue Y., 1996, ApJ, 458, 120
Sofue Y., Fujimoto M., Wielebinski R., 1986, ARA&A, 24, 459
Sukumar S., Allen R. J., 1989, Nature, 340, 537
Syer D., Tremaine S., 1996, MNRAS, 281, 925
Tacconi L. J., Young J.S., 1989, ApJS, 71, 455
Toomre A., 1963, ApJ, 138, 385
Toomre A., 1977, ARA&A, 15, 437
Vandervoort P.O., 1982, ApJ, 256, L41
Vandervoort P.O., 1983, ApJ, 273, 511
Weinberg M.D., 1983, ApJ, 271, 595
Weinberg M.D., Tremaine S., 1983, ApJ, 271, 586
Yabushita S., 1966, MNRAS, 133, 247
Zang T.A., 1976, The Stability of a Model Galaxy, Ph.D. thesis, Mass. Inst. Technol., Cambridge, Mass.

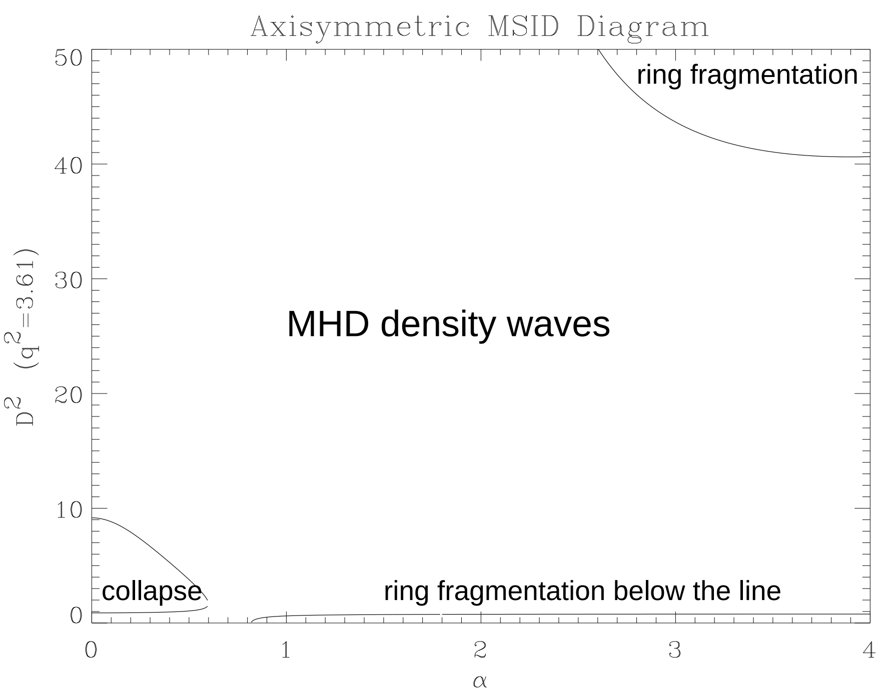
Axisymmetric MSID Diagram
ring fragmentation
MHD density waves
collapse
ring fragmentation below the line
D2 (q2=3.61)
α
0
10
20
30
40
50
1
2
3
4

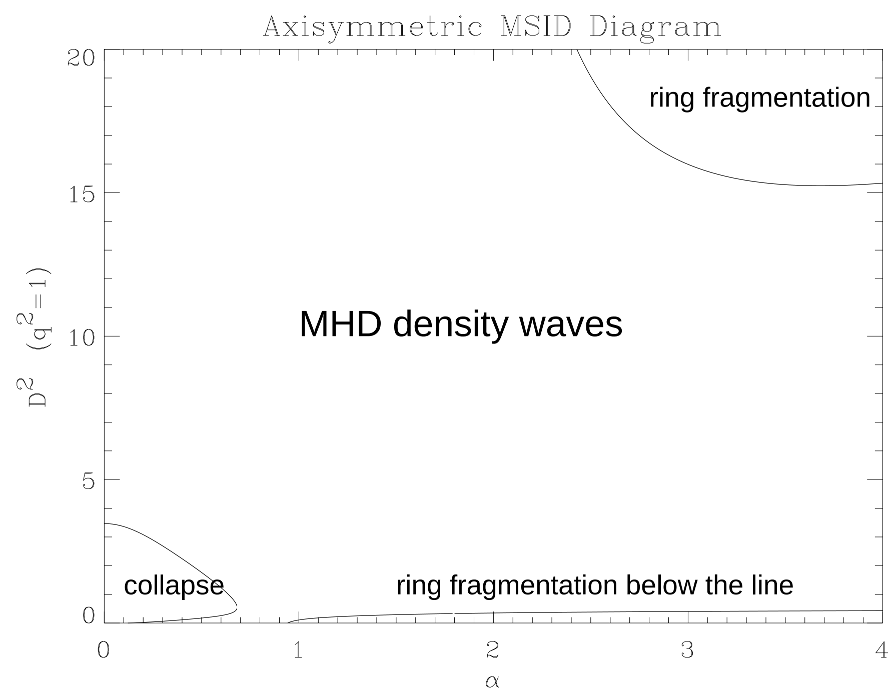
Axisymmetric MSID Diagram
ring fragmentation
MHD density waves
collapse
ring fragmentation below the line
D^2 $(q^2=1)$
α
0
5
10
15
20
0
1
2
3
4

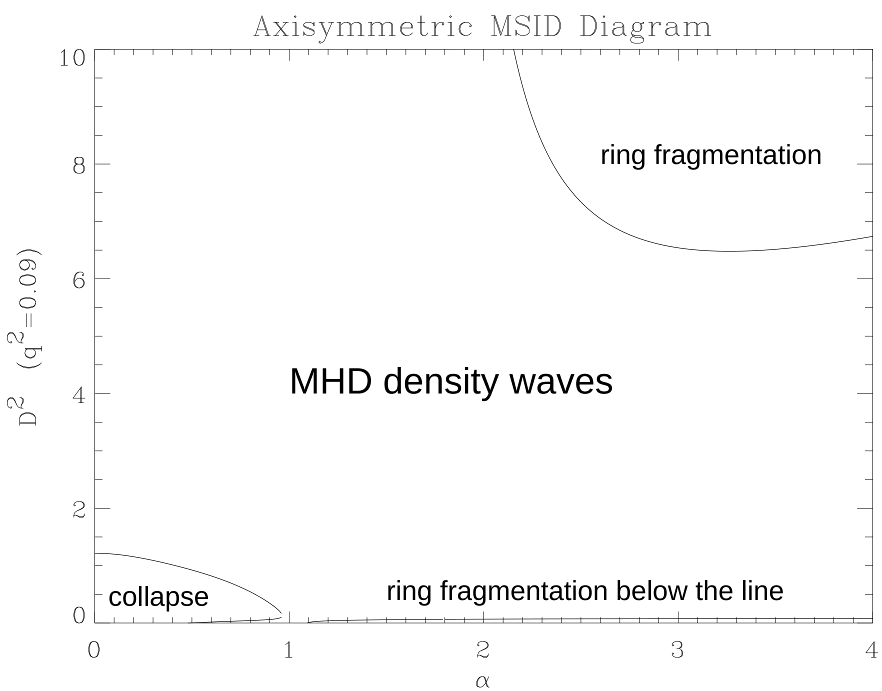
Axisymmetric MSID Diagram
ring fragmentation
MHD density waves
collapse
ring fragmentation below the line
D2 (q2=0.09)
α
0
1
2
3
4
0
2
4
6
8
10